

trisomic cells. In this regard, if trisomic cells may be present in a certain fraction of buccal cells and placental tissue, the full upid(7)mat cells would still account for a relatively major fraction of buccal cells and a relatively minor fraction of the placental cells. While such a variation in the frequency of the full upid(7)mat cells among different tissues would primarily be a stochastic event, it should be pointed out that human genetic studies are usually performed for leukocytes. Indeed, if the upid(7)mat cells were barely present in leukocytes, the mosaic upid(7)mat would not have been detected. Such a bias in human studies would more or less be relevant to the relative predominance of the full upid(7)mat cells in leukocytes.

Two findings are noteworthy with regard to clinical features of this patient. First, this patient had relatively mild SRS phenotype with speech delay and feeding difficulty. Since such clinical features are grossly consistent with those of patients with upd(7)mat [Hitchins et al., 2001; Kotzot, 2008], it is inferred that the upid(7)mat cells accounted for a considerable fraction of body cells relevant to the development of SRS phenotype. Second, the placental size remained within the normal range. This would be consistent with the relative paucity of the upid(7)mat cells in the placenta.

In summary, we observed mosaic upid(7)mat in a patient with SRS. Further studies will identify mosaic upd(7)mat with or without demonstrable trisomy 7 in patients with relatively mild SRS-like phenotype.

#### ACKNOWLEDGMENTS

This work was supported by the Grant-in-Aid for Scientific Research (A) (22249010) from the Japan Society for the Promotion of Science (JSPS), by the Grants for Health Research on Children, Youth, and Families (H21-005) from the Ministry of Health, Labor and Welfare, and by the Grant of National Center for Child Health and Development (23A-1).

#### REFERENCES

- Binder G, Begemann M, Eggermann T, Kannenberg K. 2011. Silver-Russell syndrome. *Best Pract Res Clin Endocrinol Metab* 25:153–160.
- Chen CP, Su YN, Chern SR, Hwu YM, Lin SP, Hsu CH, Tsai FJ, Wang TY, Wu PC, Lee CC, Chen YT, Chen LF, Wang W. 2010. Mosaic trisomy 7 at amniocentesis: Prenatal diagnosis and molecular genetic analyses. *Taiwan J Obstet Gynecol* 49:333–340.
- Coan PM, Burton GJ, Ferguson-Smith AC. 2005. Imprinted genes in the placenta: A review. *Placenta* 26:S10–S20.
- Eggermann T. 2010. Russell–Silver syndrome. *Am J Med Genet Part C* 154C:355–364.
- Hitchins MP, Stanier P, Preece MA, Moore GE. 2001. Silver-Russell syndrome: A dissection of the genetic aetiology and candidate chromosomal regions. *J Med Genet* 38:810–819.
- Kagami M, Yamazawa K, Matsubara K, Matsuo N, Ogata T. 2008. Placentomegaly in paternal uniparental disomy for human chromosome 14. *Placenta* 29:760–761.
- Kalousek DK, Howard-Peebles PN, Olson SB, Barrett IJ, Dorfmann A, Black SH, Schulman JD, Wilson RD. 1991. Confirmation of CVS mosaicism in term placentae and high frequency of intrauterine growth retardation association with confined placental mosaicism. *Prenat Diagn* 11:743–750.
- Kotzot D. 2008. Maternal uniparental disomy 7 and Silver–Russell syndrome—Clinical update and comparison with other subgroups. *Eur J Med Genet* 51:444–451.
- Miozzo M, Grati FR, Bulfamante G, Rossella F, Cribiù M, Radaelli T, Cassani B, Persico T, Cetin I, Pardi G, Simoni G. 2011. Post-zygotic origin of complete maternal chromosome 7 isodisomy and consequent loss of placental *PEG1/MEST* expression. *Placenta* 22:813–821.
- Petit F, Holder-Espinasse M, Duban-Bedu B, Bouquillon S, Boute-Benejean O, Bazin A, Rouland V, Manouvrier-Hanu S, Delobel B. 2011. Trisomy 7 mosaicism prenatally misdiagnosed and maternal uniparental disomy in a child with pigmentary mosaicism and Russell–Silver syndrome. *Clin Genet* [Epub ahead of print], PHID: 21204802.
- Russell A. 1954. A syndrome of intra-uterine dwarfism recognizable at birth with cranio-facial dysostosis, disproportionately short arms and other anomalies. *Proc R Soc Med* 47:1040–1044.
- Silver HK, Kiyasu W, George J, Deamer WC. 1953. Syndrome of congenital hemihypertrophy, shortness of stature, and elevated urinary gonadotrophins. *Pediatrics* 12:368–375.
- Thiede C, Prange-Krex G, Freiberg-Richter J, Bornhäuser M, Ehninger G. 2000. Buccal swabs but not mouthwash samples can be used to obtain pretransplant DNA fingerprints from recipients of allogeneic bone marrow transplants. *Bone Marrow Transplant* 25:575–577.
- Yamazawa K, Kagami M, Nagai T, Kondoh T, Onigata K, Maeyama K, Hasegawa T, Hasegawa Y, Yamazaki T, Mizuno S, Miyoshi Y, Miyagawa S, Horikawa R, Matsuoka K, Ogata T. 2008a. Molecular and clinical findings and their correlations in Silver-Russell syndrome: Implications for a positive role of IGF2 in growth determination and differential imprinting regulation of the *IGF2-H19* domain in bodies and placentas. *J Mol Med* 86:1171–1181.
- Yamazawa K, Kagami M, Ogawa M, Horikawa R, Ogata T. 2008b. Placental hypoplasia in maternal uniparental disomy for chromosome 7. *Am J Med Genet Part A* 146A:514–516.
- Yamazawa K, Nakabayashi K, Kagami M, Sato T, Saitoh S, Horikawa R, Hizuka N, Ogata T. 2010. Parthenogenetic chimaerism/mosaicism with a Silver-Russell syndrome-like phenotype. *J Med Genet* 47:782–785.

ARTICLE

# Relative frequency of underlying genetic causes for the development of UPD(14)pat-like phenotype

Masayo Kagami<sup>1</sup>, Fumiko Kato<sup>1</sup>, Keiko Matsubara<sup>1</sup>, Tomoko Sato<sup>1</sup>, Gen Nishimura<sup>2</sup> and Tsutomu Ogata<sup>\*,1,3</sup>

Paternal uniparental disomy 14 (UPD(14)pat) results in a unique constellation of clinical features, and a similar phenotypic constellation is also caused by microdeletions involving the *DLK1-MEG3* intergenic differentially methylated region (IG-DMR) and/or the *MEG3-DMR* and by epimutations (hypermethylations) affecting the DMRs. However, relative frequency of such underlying genetic causes remains to be clarified, as well as that of underlying mechanisms of UPD(14)pat, that is, trisomy rescue (TR), gamete complementation (GC), monosomy rescue (MR), and post-fertilization mitotic error (PE). To examine this matter, we sequentially performed methylation analysis, microsatellite analysis, fluorescence *in situ* hybridization, and array-based comparative genomic hybridization in 26 patients with UPD(14)pat-like phenotype. Consequently, we identified UPD(14)pat in 17 patients (65.4%), microdeletions of different patterns in 5 patients (19.2%), and epimutations in 4 patients (15.4%). Furthermore, UPD(14)pat was found to be generated through TR or GC in 5 patients (29.4%), MR or PE in 11 patients (64.7%), and PE in 1 patient (5.9%). Advanced maternal age at childbirth ( $\geq 35$  years) was predominantly observed in the MR/PE subtype. The results imply that the relative frequency of underlying genetic causes for the development of UPD(14)pat-like phenotype is different from that of other imprinting disorders, and that advanced maternal age at childbirth as a predisposing factor for the generation of nullisomic oocytes through non-disjunction at meiosis 1 may be involved in the development of MR-mediated UPD(14)pat.

*European Journal of Human Genetics* (2012) 20, 928–932; doi:10.1038/ejhg.2012.26; published online 22 February 2012

**Keywords:** genetic cause; maternal age effect; monosomy rescue; UPD(14)pat subtype

## INTRODUCTION

Human chromosome 14q32.2 carries a  $\sim 1.2$  Mb imprinted region with the germline-derived primary *DLK1-MEG3* intergenic differentially methylated region (IG-DMR) and the post-fertilization-derived secondary *MEG3-DMR*, together with multiple imprinted genes.<sup>1,2</sup> Both DMRs are methylated after paternal transmission and unmethylated after maternal transmission in the body, whereas in the placenta the IG-DMR alone remains as a DMR and the *MEG3-DMR* is rather hypomethylated irrespective of the parental origin.<sup>2,3</sup> Furthermore, it has been shown that the unmethylated IG-DMR and *MEG3-DMR* of maternal origin function as the imprinting centers in the placenta and the body, respectively, and that the IG-DMR acts as an upstream regulator for the methylation pattern of the *MEG3-DMR* in the body but not in the placenta.<sup>3</sup>

As a result of the presence of the imprinted region, paternal uniparental disomy 14 (UPD(14)pat) (OMIM #608149) causes a unique constellation of body and placental phenotypes such as characteristic face, bell-shaped small thorax, abdominal wall defect, polyhydramnios, and placentomegaly.<sup>2,4,5</sup> Furthermore, consistent with the essential role of the DMRs in the imprinting regulation, microdeletions and epimutations affecting the IG-DMR or both DMRs of maternal origin result in UPD(14)pat-like phenotype in both the body and the placenta, whereas a microdeletion involving the

maternally inherited *MEG3-DMR* alone leads to UPD(14)pat-like phenotype in the body, but not in the placenta.<sup>2,3</sup>

Of the three underlying genetic causes for UPD(14)pat-like phenotype (UPD(14)pat, microdeletions, and epimutations), UPD(14)pat is primarily generated by four mechanisms, that is, trisomy rescue (TR), gamete complementation (GC), monosomy rescue (MR), and post-fertilization mitotic error (PE).<sup>6</sup> TR refers to a condition in which chromosome 14 of maternal origin is lost from a zygote with trisomy 14 formed by fertilization between a disomic sperm and a normal oocyte. GC results from fertilization of a disomic sperm with a nullisomic oocyte. MR refers to a condition in which chromosome 14 of paternal origin is replicated in a zygote with monosomy 14 formed by fertilization between a normal sperm and a nullisomic oocyte. PE is an event after formation of a normal zygote. In this regard, a nullisomic oocyte specific to GC and MR is produced by non-disjunction at meiosis 1 (M1) or meiosis 2 (M2), and non-disjunction at M1 is known to increase with maternal age, probably because of a long-term (10–50 years) meiotic arrest at prophase 1.<sup>7</sup>

However, relative frequency of the genetic causes for UPD(14)pat-like phenotype remains to be determined, as well as that of underlying mechanisms for the generation of UPD(14)pat. Here, we report our data on this matter, and discuss the difference in the relative frequency

<sup>1</sup>Department of Molecular Endocrinology, National Research Institute for Child Health and Development, Tokyo, Japan; <sup>2</sup>Department of Radiology, Tokyo Metropolitan Children's Medical Center, Fuchu, Japan; <sup>3</sup>Department of Pediatrics, Hamamatsu University School of Medicine, Hamamatsu, Japan

\*Correspondence: Professor T Ogata, Department of Pediatrics, Hamamatsu University School of Medicine, Hamamatsu 431-3192, Japan. Tel: +81 53 435 2310; Fax: +81 53 435 2312; E-mail: tomogata@hama-med.ac.jp

Received 23 May 2011; revised 10 November 2011; accepted 26 December 2011; published online 22 February 2012

among imprinted disorders and the possible maternal age effect on the relative frequency.

## PATIENTS AND METHODS

### Patients

This study comprised 26 patients with UPD(14)pat-like phenotype (9 male patients and 17 female patients) (Table 1). Of the 26 patients, 18 patients have been reported previously; they consisted of nine sporadic patients with full UPD(14)pat,<sup>4,5</sup> one sporadic patient with segmental UPD(14)pat,<sup>4</sup> the proband of sibling cases and four sporadic patients with different patterns of microdeletions involving the unmethylated DMRs of maternal origin,<sup>2,3</sup> and three patients with epimutations (hypermethylations) of the two normally unmethylated DMRs of maternal origin.<sup>2</sup> The remaining eight patients were new sporadic cases.

Phenotypic findings of the 26 patients are summarized in Supplementary Table 1; detailed clinical features of patients 6 and 16–25 are as described previously,<sup>2–4</sup> and those of the eight new patients 3, 5, 10–14, and 26 are shown in Supplementary Table 2, together with those of patients 1, 2, 4, 7–9, and 15 in whom detailed phenotypes were not described in the previous report.<sup>5</sup> All the 26 patients were identified shortly after birth because of the unique bell-shaped thorax with coat-hanger appearance of the ribs on roentgenograms obtained because of asphyxia. Subsequent clinical analysis revealed that 25 of the 26 patients exhibited both body and placental UPD(14)pat-like phenotype, whereas the remaining one previously reported patient (patient 22) manifested body, but not placental, UPD(14)pat-like phenotype.<sup>3</sup> The karyotype was found to be normal in 25 patients, although cytogenetic analysis was not performed in one previously reported patient who died of respiratory failure at 2 h of age (patient 6).<sup>4</sup> One patient (patient 15) was conceived by *in vitro* fertilization-embryo transfer.<sup>5</sup> This study was approved by the Institute Review Board Committee at the National Center for Child Health and Development, and performed after obtaining written informed consent.

### Analysis of underlying genetic causes in patients with UPD(14)pat-like phenotype

We sequentially performed methylation analysis, microsatellite analysis, and fluorescence *in situ* hybridization (FISH), using leukocyte genomic DNA samples and lymphocyte metaphase spreads of all the 26 patients with UPD(14)pat-like phenotype. The detailed methods were as reported previously.<sup>2,3</sup> In brief, methylation analysis was performed for the IG-DMR (CG4 and CG6) and the MEG3-DMR (CG7 and the CTCF-binding sites C and D) by combined bisulfite restriction analysis and bisulfite sequencing. Microsatellite analysis was performed for multiple loci on chromosome 14, by determining the sizes of PCR products obtained with fluorescently labeled forward primers and unlabeled reverse primers. FISH analysis was carried out for the IG-DMR and the MEG3-DMR using 5104-bp and 5182-bp long PCR products, respectively, together with the RP11-56612 probe for 14q12 utilized as an internal control.

In this study, furthermore, oligonucleotide array-based comparative genomic hybridization (CGH) was also performed for the imprinted region of non-UPD(14)pat patients, using a custom-build oligo-microarray containing 12 600 probes for 14q32.2–q32.3 encompassing the imprinted region and ~10 000 reference probes for other chromosomal region (4×180K format, Design ID 032112) (Agilent Technologies, Palo Alto, CA, USA). The procedure was as described in the manufacturer's instructions.

### Analysis of subtypes in patients with UPD(14)pat

UPD(14)pat subtype was determined by microsatellite analysis.<sup>8,9</sup> In brief, heterodisomy for at least one locus was regarded as indicative of TR- or GC-mediated UPD(14)pat (TR/GC subtype), whereas isodisomy for all the informative microsatellite loci was interpreted as indicative of MR- or PE-mediated UPD(14)pat (MR/PE subtype) (for details, see Supplementary Figure S1). Here, while heterodisomy and isodisomy for a pericentromeric region in the TR/GC subtype imply a disomic sperm generation through M1

**Table 1** Summary of patients examined in this study

Patient	Genetic cause	UPD(14)pat subtype	Maternal age at childbirth (years)	Paternal age at childbirth (years)	Remark	Reference
1	UPD(14)pat	TR/GC [M1]	31	35		5
2	UPD(14)pat	TR/GC [M1]	28	29		5
3	UPD(14)pat	TR/GC [M1]	29	38		This report
4	UPD(14)pat	TR/GC [M1]	36	41		5
5	UPD(14)pat	TR/GC [M2]	30	30		This report
6	UPD(14)pat	MR/PE	42	Unknown		4,5
7	UPD(14)pat	MR/PE	31	28		5
8	UPD(14)pat	MR/PE	32	33		5
9	UPD(14)pat	MR/PE	26	35		5
10	UPD(14)pat	MR/PE	38	38		This report
11	UPD(14)pat	MR/PE	26	32		This report
12	UPD(14)pat	MR/PE	41	36		This report
13	UPD(14)pat	MR/PE	30	28		This report
14	UPD(14)pat	MR/PE	39	34		This report
15	UPD(14)pat	MR/PE	42	37	Born after IVF-ET	5
16	UPD(14)pat	MR/PE	36	36		4,5
17	UPD(14)pat-seg.	PE	27	24	Segmental isodisomy	4,5
18	Microdeletion		31	34		2
19	Microdeletion		33	36		2
20	Microdeletion		28	27		2
21	Microdeletion		27	37	IG-DMR alone	3
22	Microdeletion		25	25	MEG3-DMR alone	3
23	Epimutation		35	36		2
24	Epimutation		28	26		2
25	Epimutation		27	30		2
26	Epimutation		33	33		This report

Abbreviation: IVF-ET, *in vitro* fertilization-embryo transfer using parental gametes. The microdeletions in patients 18–22 are different in size.

and M2 non-disjunction respectively,<sup>9</sup> such discrimination between M1 and M2 non-disjunctions is impossible for the development of a nullisomic oocyte. Furthermore, it is usually impossible to discriminate between TR and GC, although the presence of trisomic cells is specific to TR. Similarly, it is also usually impossible to discriminate between MR and PE, although identification of segmental isodisomy or mosaicism is unique to PE (PE subtype).

#### Analysis of parental ages

We examined parental ages at childbirth in patients of different underlying causes and different UPD(14)pat subtypes. Statistical significance of the relative frequency was examined by the Fisher's exact probability test, and that of the median age by the Mann-Whitney's *U*-test.  $P < 0.05$  was considered significant.

## RESULTS

### Analysis of underlying causes in patients with UPD(14)pat-like phenotype

For the eight new sporadic patients, methylation analysis invariably revealed hypermethylation of both DMRs, and microsatellite analysis showed UPD(14)pat in seven patients and biparentally inherited homologs of chromosome 14 in the remaining one patient (patient 26). FISH analysis for patient 26 identified two signals for the two DMRs, and subsequently performed array CGH analysis showed no evidence for genomic rearrangements (Supplementary Figure S2). Thus, patient 26 was assessed to have an epimutation affecting the two DMRs. Furthermore, the results of array CGH analysis confirmed the presence of microdeletions in patients 18–21 and the absence of a discernible microdeletion in patients 23–25 (Supplementary Figure S2) (array CGH analysis was not performed in patient 22 with a 4303-bp microdeletion<sup>3</sup> because of the lack of DNA sample available). Thus, together with our previous data, all the 26 patients with UPD(14)pat-like phenotype had genetic alteration involving the imprinted region on chromosome14q32.2.

Consequently, the 26 patients with UPD(14)pat-like phenotype were classified as follows: (1) 16 sporadic patients with full UPD(14)pat and 1 sporadic patient with segmental UPD(14)pat (UPD(14)pat group); (2) the proband of the sibling cases and two sporadic patients with different patterns of microdeletions involving the two DMRs, one sporadic patient with a microdeletion involving the IG-DMR alone in whom the *MEG3*-DMR was epimutated, and one patient with a microdeletion involving the *MEG3*-DMR alone (deletion group); and (3) four patients with epimutations (hypermethylations) of both DMRs (epimutation group) (Figure 1 and Table 1).

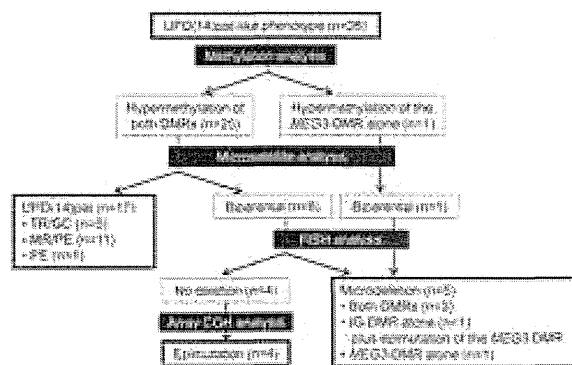


Figure 1 Classification of 26 patients with UPD(14)pat-like phenotype.

### Analysis of subtypes in patients with UPD(14)pat

Heterozygosity for at least one locus indicative of TR/GC subtype was identified in five patients (patients 1–5), and the disomic pattern of pericentromeric region indicated M1 non-disjunction in patients 1–4 and M2 non-disjunction in patient 5. Full isodisomy consistent with MR/PE subtype was detected in 11 patients (patients 6–16), and segmental isodisomy unique to PE subtype was revealed in 1 patient (patient 17) (Table 1, Figure 1, and Supplementary Figure S3).

#### Analysis of parental ages

The distribution of parental ages at childbirth is shown in Figure 2. The advanced maternal age at childbirth ( $\geq 35$  years) was predominantly observed in the MR/PE subtype of UPD(14)pat. Furthermore, while the relative frequency of aged mothers ( $\geq 35$  years) did not show a significant difference between the MR/PE subtype of UPD(14)pat (6/11) and (i) other subtypes of UPD(14)pat (1/6) ( $P=0.159$ ), (ii) deletion group (0/5) ( $P=0.057$ ), and (iii) epimutation group (1/4) ( $P=0.338$ ), it was significantly different between the MR/PE subtype and the sum of other subtypes of UPD(14)pat, deletion group, and epimutation group (2/15) ( $P=0.034$ ). Similarly, while the median maternal age did not show a significant difference between the MR/PE subtype of UPD(14)pat (36 years) vs (i) other subtypes of UPD(14)pat (29.5 years) ( $P=0.118$ ), (ii) deletion type (28 years) ( $P=0.088$ ), and (iii) epimutation type (30.5 years) ( $P=0.295$ ), it was significantly different between the MR/PE subtype of UPD(14)pat and the sum of other subtypes of UPD(14)pat, deletion group, and epimutation group (29 years) ( $P=0.045$ ).

The paternal ages were similar irrespective of the genetic causes and the UPD(14)pat subtypes. In addition, the median paternal age was comparable between the TR/GC subtype of UPD(14)pat that postulates the production of a disomic sperm (35.0 years) and the sum of other subtypes of UPD(14)pat, deletion group, and epimutation group that assumes the production of a normal sperm (33.5 years) ( $P=0.322$ ).

## DISCUSSION

This study revealed that the UPD(14)pat-like phenotype was caused by UPD(14)pat in 65.4% of patients, by microdeletions in 19.2% of patients, and by epimutations in 15.4% of patients. Although the relative frequency of underlying genetic factors for the development of UPD(14)pat-like phenotype has been reported previously,<sup>10</sup> most data are derived from our previous publications. Thus, the present results are regarded as the updated and extended data on the relative frequency. For the relative frequency, it is notable that 25 of the 26 patients were confirmed to have normal karyotype, although chromosome analysis was not performed in patient 6. Thus, while Robertsonian translocations involving chromosome 14 is known to be a

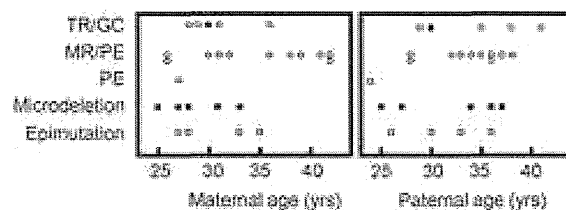


Figure 2 The distribution of parental ages at childbirth according to the underlying genetic causes for the development of UPD(14)pat-like phenotype and UPD(14)pat subtypes. Of the five plots for the TR/GC subtype, open and black circles indicate the TR/GC subtype due to non-disjunction at paternal M1 and M2, respectively.

predisposing factor for the occurrence of UPD(14)pat,<sup>11–16</sup> such a possible chromosomal effect has been excluded in nearly all patients examined in this study.

The relative frequency of underlying causes has also been reported in other imprinting disorders.<sup>8,17–19</sup> The data are summarized in Table 2 (a similar summary has also been reported recently by Hoffmann *et al*).<sup>10</sup> In particular, the results in patients with normal karyotype are available in Prader–Willi syndrome (PWS).<sup>8</sup> Furthermore, PWS is also known to be caused by UPD, microdeletions, and epimutations affecting a single imprinting region,<sup>8,19</sup> although Silver–Russell syndrome and Beckwith–Wiedemann syndrome (BWS) can result from perturbation of at least two imprinted regions,<sup>17,18</sup> and BWS and Angelman syndrome can occur as a single gene disorder.<sup>17,19</sup> Thus, it is notable that the relative frequency of underlying causes is quite different between patients with UPD(14)pat-like phenotype and those with PWS.<sup>8,19</sup> This would primarily be due to the presence of low copy repeats flanking the imprinted region on chromosome 15, because chromosomal deletions are prone to occur in regions harboring such repeat sequences.<sup>20</sup> Indeed, two types of microdeletions mediated by such low copy repeats account for a vast majority of microdeletions in patients with PWS,<sup>21</sup> whereas the microdeletions identified in patients with UPD(14)pat-like phenotype are different to each other. This would explain why microdeletions are less frequent and UPD and epimutations are more frequent in patients with UPD(14)pat-like phenotype than in those with PWS.

Advanced maternal age at childbirth was predominantly observed in the MR/PE subtype. This may imply the relevance of advanced maternal age to the development of MR-mediated UPD(14)pat, because the generation of nullisomic oocytes through M1 non-disjunction is a maternal age-dependent phenomenon.<sup>22</sup> Although no paternal age effect was observed, this is consistent with the previous data indicating no association of advanced paternal age with a meiotic error.<sup>23</sup> For the maternal age effect, however, several matters should be pointed out: (1) the number of analyzed patients is small, although it is very difficult to collect a large number of patients in this extremely rare disorder; (2) of the MR/PE subtype, the advanced maternal age is a risk factor for the generation of MR-mediated UPD(14)pat, but not for the development of PE-mediated UPD(14)pat; (3) it is impossible to discriminate between maternal age-dependent M1 non-disjunction

and maternal age-independent M2 non-disjunction in the MR and GC subtypes (however, GC must be extremely rare, because it requires the concomitant occurrence of a nullisomic oocyte and a disomic sperm); (4) of the TR/GC subtype, the advanced maternal age is a risk factor for the generation of GC-mediated UPD(14)pat, but not for the development of TR-mediated UPD(14)pat; and (5) if a cryptic recombination(s) might remain undetected in some patients with apparently full isodisomy, this argues that such patients actually have TR- or GC-mediated UPD(14)pat rather than MR- or PE-mediated UPD(14)pat. Thus, further studies are required to examine the maternal age effect on the generation of MR-mediated UPD(14)pat. In addition, while a relationship is unlikely to exist between advanced maternal age and microdeletions and epimutations, this notion would also await further investigations.

Such a maternal age effect is also expected in the TR/GC subtype maternal UPDs after M1 non-disjunction, because the generation of disomic oocytes through M1 non-disjunction is also a maternal age-dependent phenomenon.<sup>7</sup> Indeed, such a maternal age effect has been shown for PWS patients with normal karyotype; the maternal age at childbirth was significantly higher in patients with heterodisomy for a very pericentromeric region indicative of TR/GC subtype UPD(15)mat after M1 non-disjunction than in those with other genetic causes.<sup>8,9</sup> For various chromosomes other than chromosome 15, furthermore, since maternal age at childbirth is higher in patients with maternal heterodisomy than in those with maternal isodisomy,<sup>24</sup> this would also argue for maternal age effect on the development of maternal UPDs. However, in the previous studies on maternal UPDs other than UPD(15)mat, the available data are quite insufficient to assess the maternal age effect. For example, although a relatively large number of patients with UPD(14)mat phenotype have been reported in the literature (reviewed in reference Hoffmann *et al*),<sup>10</sup> we could identify only six UPD(14)mat patients with normal karyotype in whom maternal age at childbirth was documented and microsatellite analysis was performed.<sup>25–30</sup> Furthermore, the microsatellite data are insufficient to identify the subtype of UPD(14)mat and to distinguish between M1 and M2 non-disjunction in the TR/GC subtype. Thus, while the maternal age at childbirth may be advanced in five patients with apparently TR/GC-mediated UPD(14)mat (27, 35, 37, 41, and 44 years)<sup>25–27,29,30</sup> (the maternal age at childbirth in the remaining one

**Table 2** Relative frequency of genetic mechanisms in imprinting disorders

	UPD(14)pat-like phenotype	BWS	SRS	AS	PWS
Uniparental disomy	65.4%	16%	10%	3–5%	25% (25%)
	UPD(14)pat	UPD(11)pat (mosaic)	UPD(7)mat	UPD(15)pat	UPD(15)mat
Cryptic deletion	19.2%	Rare	—	70%	70% (72%)
Cryptic duplication	—	—	Rare	—	—
<i>Epimutation</i>					
Hypermethylation	15.4%	9%	—	—	2–5% (2%)
Affected DMR	IG-DMR/MEG3-DMR	H19-DMR	—	—	SNRPN-DMR
Hypomethylation	—	44%	> 38%	2–5%	—
Affected DMR	—	KvDMR1	H19-DMR	SNRPN-DMR	—
<i>Gene mutation</i>					
Mutated gene	—	5%	—	10–15%	—
	—	CDKN1C	—	UBE3A	—
Unknown	—	25%	> 40%	10%	—
Reference	This study	17	18	19	8, 19

Abbreviations: AS, Angelman syndrome; BWS, Beckwith–Wiedemann syndrome; PWS, Prader–Willi syndrome; SRS, Silver–Russell syndrome.

Patients with abnormal karyotypes are included in BWS and AS, and not included in SRS. In PWS, the data including patients with abnormal karyotypes are shown, and those from patients with normal karyotype alone are depicted in parentheses.

patient with apparently MR/PE-mediated UPD(14)mat is 40 years),<sup>28</sup> the notion of a maternal age effect awaits further investigations for UPD(14)mat.

Finally, it appears to be worth pointing out that methylation analysis invariably revealed hypermethylated DMR(s) in all the 26 patients who were initially ascertained because of bell-shaped thorax with coat-hanger appearance of the ribs. This indicates that methylation analysis of the DMRs can be utilized for a screening of this condition, and that the constellation of clinical features in the UPD(14)pat-like phenotype, especially the bell-shaped thorax with coat-hanger appearance of the ribs, is highly unique to patients with UPD(14)pat-like phenotype.

In summary, this study confirms the relative frequency of underlying genetic causes for the UPD(14)pat phenotype and reveals the relative frequency of UPD(14)pat subtypes. Furthermore, the results emphasize the difference in the relative frequency of underlying genetic causes among imprinted disorders, and may support a possible maternal age effect on the generation of the nullisomic oocyte mediated UPD(14)pat. Further studies will permit a more precise assessment on these matters.

#### CONFLICT OF INTEREST

The authors declare no conflict of interest.

#### ACKNOWLEDGEMENTS

We thank Drs Kenji Kurosawa, Michiko Hayashidani, Toshio Takeuchi, Shinya Tanaka, Mika Noguch, Kouji Masumoto, Takeshi Utsunomiya, Yumiko Komatsu, Hirofumi Ohashi, Maureen J O'Sullivan, Andrew J Green, Yoshiyuki Watabe, Tsuyako Iwai, Hitoshi Kawato, Miho Torikai, Akiko Yamamoto, Nobuhiro Suzumori, Makoto Kuwajima, Hiroshi Yoshihashi, Yoriko Watanabe, and Jin Nishimura for material sampling and phenotype assessment. This work was supported by Grants for Research on Intractable Diseases (H22-161) and for Health Research on Children, Youth and Families (H21-005) from the Ministry of Health, Labor and Welfare, by Grants-in-Aid for Scientific Research (A) (22249010) and (B) (21028026) from the Japan Society for the Promotion of Science (JSPS), by Grants from Takeda Science Foundation and from Kanehara Foundation, and by the Grant for National Center for Child Health and Development (23A-1).

- da Rocha ST, Edwards CA, Ito M, Ogata T, Ferguson-Smith AC: Genomic imprinting at the mammalian Dkl1-Dio3 domain. *Trends Genet* 2008; **24**: 306–316.
- Kagami M, Sekita Y, Nishimura G *et al*: Deletions and epimutations affecting the human 14q32.2 imprinted region in individuals with paternal and maternal upd(14)-like phenotypes. *Nat Genet* 2008; **40**: 237–242.
- Kagami M, O'Sullivan MJ, Green AJ *et al*: The IG-DMR and the MEG3-DMR at human chromosome 14q32.2: hierarchical interaction and distinct functional properties as imprinting control centers. *PLoS Genet* 2010; **6**: e1000992.
- Kagami M, Nishimura G, Okuyama T *et al*: Segmental and full paternal isodisomy for chromosome 14 in three patients: narrowing the critical region and implication for the clinical features. *Am J Med Genet A* 2005; **138A**: 127–132.
- Kagami M, Yamazawa K, Matsubara K, Matsuo N, Ogata T: Placentomegaly in paternal uniparental disomy for human chromosome 14. *Placenta* 2008; **29**: 760–761.
- Shaffer LG, Agan N, Goldberg JD, Ledbetter DH, Longshore JW, Cassidy SB: American College of Medical Genetics statement of diagnostic testing for uniparental disomy. *Genet Med* 2001; **3**: 206–211.
- Jones KT: Meiosis in oocytes: predisposition to aneuploidy and its increased incidence with age. *Hum Reprod Update* 2008; **14**: 143–158.
- Matsubara K, Murakami N, Nagai T, Ogata T: Maternal age effect on the development of Prader-Willi syndrome resulting from upd(15)mat through meiosis 1 errors. *J Hum Genet* 2011; **56**: 566–571.
- Robinson WP, Christian SL, Kuchinka BD *et al*: Somatic segregation errors predominantly contribute to the gain or loss of a paternal chromosome leading to uniparental disomy for chromosome 15. *Clin Genet* 2000; **57**: 349–358.
- Hoffmann K, Heller R: Uniparental disomies 7 and 14. *Best Pract Res Clin Endocrinol Metab* 2011; **25**: 77–100.
- Wang JC, Passage MB, Yen PH, Shapiro LJ, Mohandas TK: Uniparental heterodisomy for chromosome 14 in a phenotypically abnormal familial balanced 13/14 Robertsonian translocation carrier. *Am J Hum Genet* 1991; **48**: 1069–1074.
- Papenhausen PR, Mueller OT, Johnson VP, Sutcliffe M, Diamond TM, Kousseff BG: Uniparental isodisomy of chromosome 14 in two cases: an abnormal child and a normal adult. *Am J Med Genet* 1995; **59**: 271–275.
- Cotter PD, Kaffe S, McCurdy LD, Jhaveri M, Willner JP, Hirschhorn K: Paternal uniparental disomy for chromosome 14: a case report and review. *Am J Med Genet* 1997; **70**: 74–79.
- Yano S, Li L, Owen S, Wu S, Tran T: A further delineation of the paternal uniparental disomy (UPD14): the fifth reported liveborn case. *Am J Hum Genet* 2001; **69** (Suppl): A739.
- Kurosawa K, Sasaki H, Sato Y *et al*: Paternal UPD14 is responsible for a distinctive malformation complex. *Am J Med Genet A* 2002; **110**: 268–272.
- McGowan KD, Weiser JJ, Horwitz J *et al*: The importance of investigating for uniparental disomy in prenatally identified balanced acrocentric rearrangements. *Prenat Diagn* 2002; **22**: 141–143.
- Sasaki K, Soejima H, Higashimoto K *et al*: Japanese and North American/European patients with Beckwith-Wiedemann syndrome have different frequencies of some epigenetic and genetic alterations. *Eur J Hum Genet* 2007; **15**: 1205–1210.
- Eggermann T: Epigenetic regulation of growth: lessons from Silver-Russell syndrome. *Endocr Dev* 2009; **14**: 10–19.
- Gurrieri F, Accadia M: Genetic imprinting: the paradigm of Prader-Willi and Angelman syndromes. *Endocr Dev* 2009; **14**: 20–28.
- Pujana MA, Nadal M, Guitart M, Armengol L, Gratacos M, Estivill X: Human chromosome 15q11-q14 regions of rearrangements contain clusters of LCR15 duplicons. *Eur J Hum Genet* 2002; **10**: 26–35.
- Varela MC, Kok F, Setian N, Kim CA, Koiffmann CP: Impact of molecular mechanisms, including deletion size, on Prader-Willi syndrome phenotype: study of 75 patients. *Clin Genet* 2005; **67**: 47–52.
- Pellestor F, Andreo B, Anahory T, Hamamah S: The occurrence of aneuploidy in human: lessons from the cytogenetic studies of human oocytes. *Eur J Med Genet* 2006; **49**: 103–116.
- Sloter E, Nath J, Eskenazi B, Wyrobek AJ: Effects of male age on the frequencies of germinal and heritable chromosomal abnormalities in humans and rodents. *Fertil Steril* 2004; **81**: 925–943.
- Kotzot D: Advanced parental age in maternal uniparental disomy (UPD): implications for the mechanism of formation. *Eur J Hum Genet* 2004; **12**: 343–346.
- Fokstuen S, Ginsburg C, Zachmann M, Schinzel A: Maternal uniparental disomy 14 as a cause of intrauterine growth retardation and early onset of puberty. *J Pediatr* 1999; **134**: 689–695.
- Hordijk R, Wierenga H, Scheffer H, Leegte B, Hofstra RM, Stolte-Dijkstra I: Maternal uniparental disomy for chromosome 14 in a boy with a normal karyotype. *J Med Genet* 1999; **36**: 782–785.
- Sanlaville D, Aubry MC, Dumez Y *et al*: Maternal uniparental heterodisomy of chromosome 14: chromosomal mechanism and clinical follow up. *J Med Genet* 2000; **37**: 525–528.
- Towner DR, Shaffer LG, Yang SP, Walgenbach DD: Confined placental mosaicism for trisomy 14 and maternal uniparental disomy in association with elevated second trimester maternal serum human chorionic gonadotrophin and third trimester fetal growth restriction. *Prenat Diagn* 2001; **21**: 395–398.
- Aretz S, Raff R, Woelfle J *et al*: Maternal uniparental disomy 14 in a 15-year-old boy with normal karyotype and no evidence of precocious puberty. *Am J Med Genet A* 2005; **135**: 336–338.
- Mitter D, Buiting K, von Eggeling F *et al*: Is there a higher incidence of maternal uniparental disomy 14 [upd(14)mat]? Detection of 10 new patients by methylation-specific PCR. *Am J Med Genet A* 2006; **140**: 2039–2049.



This work is licensed under the Creative Commons Attribution-NonCommercial-No Derivative Works 3.0 Unported Licence. To view a copy of this licence, visit <http://creativecommons.org/licenses/by-nc-nd/3.0/>

Supplementary Information accompanies the paper on European Journal of Human Genetics website (<http://www.nature.com/ejhg>)

# Molecular and Clinical Studies in 138 Japanese Patients with Silver-Russell Syndrome

Tomoko Fuke<sup>1,2</sup>, Seiji Mizuno<sup>3</sup>, Toshiro Nagai<sup>4</sup>, Tomonobu Hasegawa<sup>2</sup>, Reiko Horikawa<sup>5</sup>, Yoko Miyoshi<sup>6</sup>, Koji Muroya<sup>7</sup>, Tatsuro Kondoh<sup>8</sup>, Chikahiko Numakura<sup>9</sup>, Seiji Sato<sup>10</sup>, Kazuhiko Nakabayashi<sup>11</sup>, Chiharu Tayama<sup>11</sup>, Kenichiro Hata<sup>11</sup>, Shinichiro Sano<sup>1,12</sup>, Keiko Matsubara<sup>1</sup>, Masayo Kagami<sup>1</sup>, Kazuki Yamazawa<sup>1</sup>, Tsutomu Ogata<sup>1,12\*</sup>

1 Department of Molecular Endocrinology, National Research Institute for Child Health and Development, Tokyo, Japan, 2 Department of Pediatrics, Keio University School of Medicine, Tokyo, Japan, 3 Department of Pediatrics, Central Hospital, Aichi Human Service Center, Aichi, Japan, 4 Department of Pediatrics, Dokkyo Medical University Koshigaya Hospital, Saitama, Japan, 5 Division of Endocrinology and Metabolism, National Center for Child Health and Development, Tokyo, Japan, 6 Department of Pediatrics, Osaka University Graduate School of Medicine, Suita, Japan, 7 Department of Endocrinology and Metabolism, Kanagawa Children's Medical Center, Kanagawa, Japan, 8 Division of Developmental Disability, Misakaenosono Mutsumi Developmental, Medical, and Welfare Center, Isahaya, Japan, 9 Department of Pediatrics, Yamagata University School of Medicine, Yamagata, Japan, 10 Department of Pediatrics, Saitama Municipal Hospital, Saitama, Japan, 11 Department of Maternal-Fetal Biology, National Research Institute for Child Health and Development, Tokyo, Japan, 12 Department of Pediatrics, Hamamatsu University School of Medicine, Hamamatsu, Japan

## Abstract

**Background:** Recent studies have revealed relative frequency and characteristic phenotype of two major causative factors for Silver-Russell syndrome (SRS), i.e. epimutation of the *H19*-differentially methylated region (DMR) and uniparental maternal disomy 7 (upd(7)mat), as well as multilocus methylation abnormalities and positive correlation between methylation index and body and placental sizes in *H19*-DMR epimutation. Furthermore, rare genomic alterations have been found in a few of patients with idiopathic SRS. Here, we performed molecular and clinical findings in 138 Japanese SRS patients, and examined these matters.

**Methodology/Principal Findings:** We identified *H19*-DMR epimutation in cases 1–43 (group 1), upd(7)mat in cases 44–52 (group 2), and neither *H19*-DMR epimutation nor upd(7)mat in cases 53–138 (group 3). Multilocus analysis revealed hyper- or hypomethylated DMRs in 2.4% of examined DMRs in group 1; in particular, an extremely hypomethylated *ARHI*-DMR was identified in case 13. Oligonucleotide array comparative genomic hybridization identified a ~3.86 Mb deletion at chromosome 17q24 in case 73. Epigenotype-phenotype analysis revealed that group 1 had more reduced birth length and weight, more preserved birth occipitofrontal circumference (OFC), more frequent body asymmetry and brachydactyly, and less frequent speech delay than group 2. The degree of placental hypoplasia was similar between the two groups. In group 1, the methylation index for the *H19*-DMR was positively correlated with birth length and weight, present height and weight, and placental weight, but with neither birth nor present OFC.

**Conclusions/Significance:** The results are grossly consistent with the previously reported data, although the frequency of epimutations is lower in the Japanese SRS patients than in the Western European SRS patients. Furthermore, the results provide useful information regarding placental hypoplasia in SRS, clinical phenotypes of the hypomethylated *ARHI*-DMR, and underlying causative factors for idiopathic SRS.

**Citation:** Fuke T, Mizuno S, Nagai T, Hasegawa T, Horikawa R, et al. (2013) Molecular and Clinical Studies in 138 Japanese Patients with Silver-Russell Syndrome. PLoS ONE 8(3): e60105. doi:10.1371/journal.pone.0060105

**Editor:** Monica Miozzo, Università degli Studi di Milano, Italy

**Received:** September 7, 2012; **Accepted:** February 21, 2013; **Published:** March 22, 2013

**Copyright:** © 2013 Fuke et al. This is an open-access article distributed under the terms of the Creative Commons Attribution License, which permits unrestricted use, distribution, and reproduction in any medium, provided the original author and source are credited.

**Funding:** This work was funded by Grants-in-Aid for Scientific Research (A) (22249010) and Research (B) (21028026) from the Japan Society for the Promotion of Science (<http://www.jsps.go.jp/english/index.html>), by Grant for Research on Rare and Intractable Diseases (H24-042) from the Ministry of Health, Labor and Welfare (<http://www.mhlw.go.jp/english/>), and by Grant for National Center for Child Health and Development (23A-1) (<http://www.ncchd.go.jp/English/EnglishTop.htm>). The funders had no role in study design, data collection and analysis, decision to publish, or preparation of the manuscript.

**Competing Interests:** The authors have declared that no competing interests exist.

\* E-mail: tomogata@hama-med.ac.jp

## Introduction

Silver-Russell syndrome (SRS) is a rare congenital developmental disorder characterized by pre- and postnatal growth failure, relative macrocephaly, triangular face, hemihypotrophy, and fifth-finger clinodactyly [1]. Recent studies have shown that epimutation (hypomethylation) of the paternally derived differentially methylated region (DMR) in the upstream of *H19* (*H19*-DMR) on

chromosome 11p15.5 and maternal uniparental disomy for chromosome 7 (upd(7)mat) account for ~45% and 5–10% of SRS patients, respectively [1,2]. In this regard, phenotypic assessment has suggested that birth length and weight are more reduced and characteristic body features are more frequent in patients with *H19*-DMR epimutation than in those with upd(7)mat, whereas developmental delay tends to be more

frequent in patients with upd(7)mat than in those with *H19*-DMR epimutation [3,4]. Furthermore, consistent with the notion that imprinted genes play an essential role in placental growth and development [5], placental hypoplasia has been found in both *H19*-DMR epimutation and upd(7)mat [4,6], although comparison of placental weight has not been performed between *H19*-DMR hypomethylation and upd(7)mat. In addition, multilocus hypo- or hypermethylation and positive correlation between methylation index (MI, the ratio of methylated clones) and body and placental sizes have been reported in patients with *H19*-DMR epimutation [4,7–9], and several types of rare genomic alterations have been identified in a few of SRS patients [1,10–12].

Here, we report on molecular and clinical findings in 138 Japanese SRS patients, and discuss on the results obtained in this study.

## Patients and Methods

### Ethics statement

This study was approved by the Institutional Review Board Committee at the National Center for Child Health and Development. The parents of the affected children and the adult patients who can express an intention by themselves have given written informed consent to participate in this study and to publish their molecular and clinical data.

### Patients

This study consisted of 138 Japanese patients (66 males and 72 females) with SRS phenotype aged 0–30 years (median 4.1 years), including 64 previously reported patients (20 patients with variable degrees of *H19*-DMR epimutation, three patients with upd(7)mat, one patient with 46,XY/46,XY,upd(7)mat mosaicism in whom upd(7)mat cells accounted for 91–92% of leukocytes and salivary cells and for 11% of placental tissue, and 40 patients of unknown cause) [4,6,13]. The 138 patients had a normal karyotype in all the  $\geq 50$  lymphocytes examined, and satisfied the selection criteria proposed by Netchine et al. [14], i.e., birth length and/or birth weight  $\leq -2$  standard deviation score (SDS) for gestational age as a mandatory criteria plus at least three of the following five features: (i) postnatal short stature ( $\leq -2$  SDS) at 2 year of age or at the nearest measure available, (ii) relative macrocephaly at birth, i.e., SDS for birth length or birth weight minus SDS for birth occipitofrontal circumference (OFC)  $\leq -1.5$ , (iii) prominent forehead during early childhood, (iv) body asymmetry, and (v) feeding difficulties during early childhood. Birth and present length/height, weight, and OFC were assessed by the gestational/postnatal age- and sex-matched Japanese reference data from the Ministry of Health, Labor, and Welfare and the Ministry of Education, Science, Sports and Culture. Placental weight was assessed by the gestational age-matched Japanese reference data [15]. Clinical features were evaluated by clinicians at different hospitals who participated in this study, using the same clinical datasheet. The SRS patients were classified into three groups by the molecular studies, i.e., those with *H19*-DMR hypomethylation (epimutation) (group 1), those with upd(7)mat (group 2), and the remaining patients (group 3).

### Primers and samples

Primers utilized in this study are shown in Table S1. Leukocyte genomic DNA samples were examined in this study.

### Methylation analysis

We performed pyrosequencing analysis for the *H19*-DMR encompassing the 6th CTCF (CCCTC-binding factor) binding site

that functions as the primary regulator for the monoallelic *IGF2* and *H19* expressions [16–18], using bisulfite treated leukocyte genomic DNA samples of all the 138 patients. The procedure was as described in the manufacturer's instructions (Qjagen, Valencia, CA, USA). In brief, a 279 bp region was PCR-amplified with a primer set (PyF and PyR) for both methylated and unmethylated clones, and a sequence primer (SP) was hybridized to a single-stranded PCR products. Subsequently, the MIs were obtained for four CpG dinucleotides (CG5–CG7 and CG9), using PyroMark Q24 (Qjagen) (the MI for CG8 was not obtained, because the “C” residue of CG8 constitutes a C/T SNP) (Figure 1A). The PyF/PyR and SP were designed by PyroMark Assay Design Software Ver2.0. While the PyF sequence contains a SNP (*rs11564736*) with a mean minor allele frequency of 5% in multiple populations, the minor allele frequency is 0% in the Japanese as well as in the Asian populations ([http://browser.1000genomes.org/Homo\\_sapiens/Variation/Population?db=core;r=11:2020801–2021801;v=rs11564736;vdb=variation;vf=7864021](http://browser.1000genomes.org/Homo_sapiens/Variation/Population?db=core;r=11:2020801–2021801;v=rs11564736;vdb=variation;vf=7864021)). Thus, we utilized this PyF.

We also carried out combined bisulfite restriction analysis (COBRA) for the *H19*-DMR. The methods were as described previously [4]. In short, a 435 bp region was PCR-amplified with a primer set (CoF and CoR) that hybridize to both methylated and unmethylated clones, and MIs were obtained for two CpG dinucleotides (CG5 and CG16) after digestion of the PCR products with methylated allele-specific restriction enzymes (*Hpy188I* and *AflIII*) (Figure 1A).

Thus, we could examine CG5 by both pyrosequencing and COBRA. While we also attempted to analyze CG16 by both methods, it was impossible to design an SP for the analysis of CG16 (although we could design an SP between CG11 and CG12, clear methylation data were not obtained for CG16, probably because of the distance between the SP and CG16).

In addition, we performed COBRA for the KvDMR1 in all the 138 patients (Figure S1A) because of the possibility that epimutation of the KvDMR1 could lead to SRS phenotype via some mechanism(s) such as overexpression of a negative growth regulator *CDKN1C* [19], and for multiple DMRs on various chromosomes in patients in whom relatively large amount of DNA samples were available, as reported previously [4,20,21]. To define the reference ranges of MIs (minimum ~ maximum), 50 control subjects were similarly studied with permission.

To screen upd(7)mat, PCR amplification was performed for the *MEST*-DMR on chromosome 7q32.2 in all the 138 patients, using methylated and unmethylated allele-specific PCR primer sets, as reported previously [6] (Figure 2A). In addition, bisulfite sequencing and direct sequencing for the primer binding sites for the *ARHI*-DMR analysis were performed in a patient (case 13) with an extremely low MI for the *ARHI*-DMR.

### Microsatellite analysis

Microsatellite analysis was performed for four loci within a ~4.5 Mb telomeric 11p region (*D11S2071*, *D11S922*, *D11S1318*, and *D11S988*) in patients with hypomethylated *H19*-DMR, to examine the possibility of upd(11p)mat involving the *H19*-DMR. Microsatellite analysis was also carried out for nine loci widely dispersed on chromosome 7 (Table S2) in patients with abnormal methylation patterns of the *MEST*-DMR, to examine the possibility of upd(7)mat and to infer the underlying causes for upd(7)mat, i.e., trisomy rescue, gamete complementation, monosomy rescue, and post-fertilization mitotic error [22]. The methods have been reported previously [4,6].

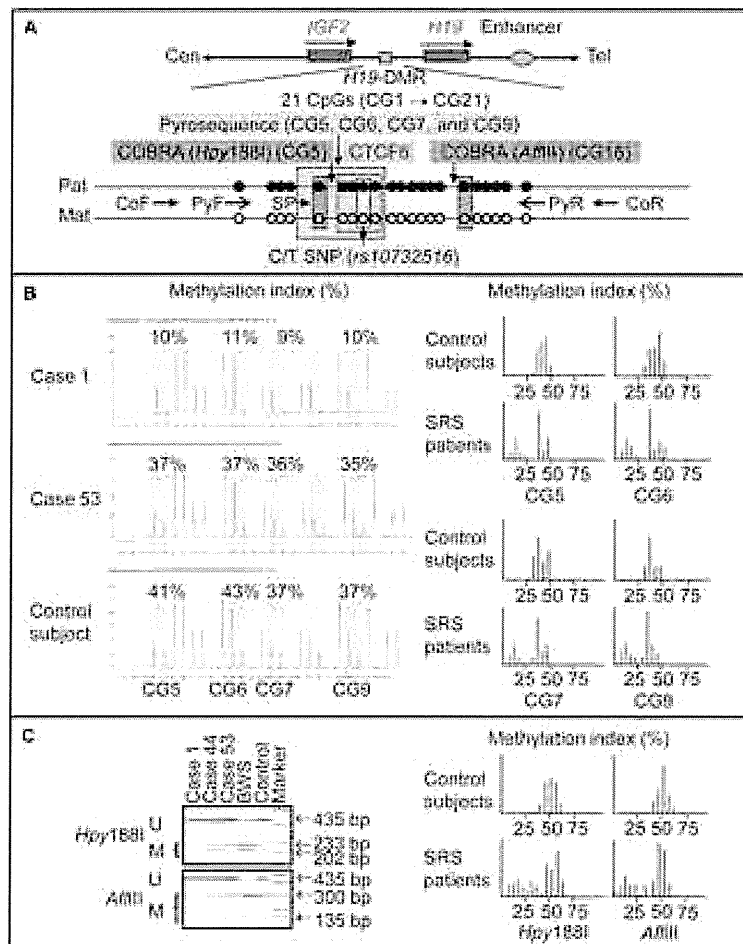


**Figure 1. Methylation analysis of the *H19*-DMR, using bisulfite-treated genomic DNA.** A. Schematic representation of a segment encompassing 21 CpG dinucleotides (CG1→CG21) within the *H19*-DMR. The cytosine residues at the CpG dinucleotides are usually methylated after paternal transmission (filled circles) and unmethylated after maternal transmission (open circles). The CTCF binding site 6 (CTCF6) is indicated with a blue rectangle; the cytosine residue at CG8 constitutes a C/T SNP (indicated with a gray rectangle). For pyrosequencing analysis, a 279 bp segment was PCR-amplified with PyF & PyR primers, and a sequence primer (SP) was hybridized to a single-stranded PCR products. Subsequently, the MIs were obtained for four CpG dinucleotides (CG5–CG7 and CG9) (indicated with a yellow rectangle). For COBRA, a 435 bp region was PCR-amplified with CoF & CoR primers, and the PCR product was digested with methylated allele-specific restriction enzymes to examine the methylation pattern of CG5 and CG16 (the PCR products is digested with *Hpy188I* when the cytosine residue at CG5 is methylated and with *AflIII* when the cytosine residue at CG16 is methylated) (indicated with orange rectangles). *IGF2* is a paternally expressed gene, and *H19* is a maternally expressed gene. The stippled ellipse indicates the enhancer for *IGF2* and *H19*. B. Pyrosequencing data. Left part: Representative results indicating the MIs for CG5–CG7 and CG9. CG5–CG7 and CG9 are hypomethylated in case 1, and similarly methylated between case 53 and a control subject. Right part: Histograms showing the distribution of the MIs (the horizontal axis: the methylation index; and the vertical axis: the patient number). Forty-three SRS patients with low MIs are shown in red. C. COBRA data. Left part: Representative findings of PCR products loaded onto a DNA 1000 LabChip (Agilent, Santa Clara, CA, USA) after digestion with *Hpy188I* or *AflIII*. U: unmethylated clone specific bands; M: methylated clone specific bands; and BWS: Beckwith-Wiedemann syndrome patient with upd(1p15)pat. Right part: Histograms showing the distribution of the MIs.

doi:10.1371/journal.pone.0060105.g001

#### Oligoarray comparative genomic hybridization (CGH)

We performed oligoarray CGH in the 138 SRS patients, using a genome-wide 4×180K Agilent platform catalog array and a custom-build high density oligoarray for the 11p15.5, 7p12.2, 12q14, and 17q24 regions where rare copy number variants have been identified in several SRS patients [1,10–12] as well as for the 7q32–qter region involved in the segmental upd(7)mat in four SRS patients [23–25]. The custom-build high density oligoarray contained 3,214 probes for 7p12.2, 434 probes for 7q32, 23,162

probes for 12q14, and 39,518 probes for 17q24, together with ~10,000 reference probes for other chromosomal region (Agilent Technologies, Palo Alto, CA, USA). The procedure was as described in the manufacturer's instructions.

#### Statistical analysis

After examining normality by  $\chi^2$  test, the variables following the normal distribution were expressed as the mean±SD, and those not following the normal distribution were expressed with the

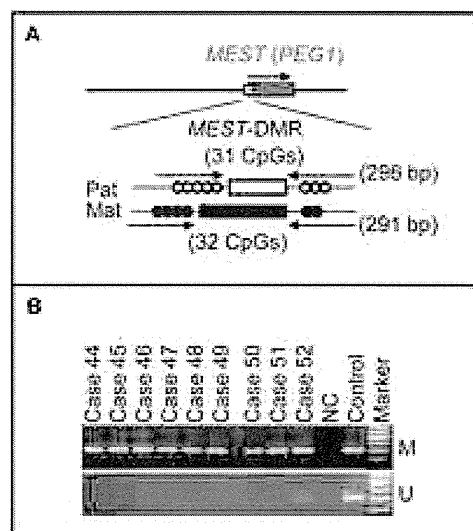


**Figure 2. Methylated and unmethylated allele-specific PCR analysis for the *MEST*-DMR.** A. Schematic representation of the *MEST*-DMR. The cytosine residues at the CpG dinucleotides are usually unmethylated after paternal transmission (open circles) and methylated after maternal transmission (filled circles). The PCR primers have been designed to hybridize either methylated or unmethylated clones. B. The results of methylation analysis with methylated and unmethylated allele-specific primers.

doi:10.1371/journal.pone.0060105.g002

median and range. Statistical significance of the mean was analyzed by Student's *t*-test or Welch's *t*-test after comparing the variances by *F* test, that of the median by Mann-Whitney's *U*-test, that of the frequency by Fisher's exact probability test, and that of the correlation by Pearson's correlation coefficient after confirming the normality of the variables.  $P < 0.05$  was considered significant.

## Results

### Identification of *H19*-DMR hypomethylation

Representative findings are shown in Figure 1B and 1C, and the MIs are summarized in Table 1. Overall, the MIs obtained by the pyrosequencing analysis tended to be lower and distributed more narrowly than those obtained by the COBRA. Despite such difference, the MIs obtained by the pyrosequencing analysis for CG5–CG7 and CG9 and by the COBRA for CG5 and CG16 were invariably below the normal range in the same 43 patients (cases 1–43) (group 1). By contrast, the MIs were almost invariably within the normal range in the remaining 95 patients, while the MIs obtained by the pyrosequencing analysis slightly (1–2%) exceeded the normal range in the same three patients (cases 136–138).

In the 43 cases of group 1, microsatellite analysis for four loci at the telomeric 11p region excluded maternal upd in 14 cases in whom parental DNA samples were available; in the remaining 29 cases, microsatellite analysis identified two alleles for at least one locus, excluding maternal uniparental isodisomy for this region. Furthermore, oligoarray CGH for the chromosome 11p15.5 region showed no copy number alteration such as duplication of maternally derived *H19*-DMR and deletion of paternally derived

**Table 1.** The methylation indices (%) for the *H19*-DMR.

	Cases 1–43	Cases 44–138	Control subjects
Pyrosequencing analysis			
CG5	4–24	35–50	33–48
CG6	5–26	36–53	34–51
CG7	4–24	35–49	30–47
CG9	5–23	34–48	30–46
COBRA			
CG5 ( <i>Hpy</i> 188I)	3.3–35.1	37.8–60.8	36.2–58.5
CG16 ( <i>Afl</i> III)	4.1–35.0	43.0–59.4	38.7–60.0

The position of examined CpG dinucleotides (CG5–7, CG9, and CG16) is shown in Figure 1A.

COBRA: combined bisulfite restriction analysis.

doi:10.1371/journal.pone.0060105.t001

*H19*-DMR. For the *KvDMR1*, the MIs of the 138 patients remained within the reference range (Fig. S1B and C).

### Identification of upd(7)mat

Methylation analysis for the *MEST*-DMR revealed that unmethylated bands were absent from eight patients and remained faint in a single patient (cases 44–52) (group 2) (Figure 2B). Subsequent microsatellite analysis confirmed upd(7)mat in the eight patients and mosaic upd(7)mat in the remaining one patient, and indicated trisomy rescue or gamete complementation type upd(7)mat in cases 44–48, monosomy rescue or post-fertilization mitotic error type upd(7)mat in cases 49–51, and post-fertilization mitotic error type mosaic upd(7)mat in case 52 (Table S2).

### Multiple DMR analysis

We examined 17 autosomal DMRs other than the *H19*-DMR in 14 patients in group 1, four patients in group 2, and 20 patients in group 3, and the *XIST*-DMR in eight female patients in group 1, one female patient in group 2, and five female patients in group 3 (Table S3). The MIs outside the reference ranges were identified in five of 14 examined cases (35.7%) and six of a total of 246 examined DMRs (2.4%) in group 1. In particular, a single case with the mean MI value of 23 obtained by the pyrosequencing analysis for CG5–CG7 and CG9 had an extremely low MI for the *ARHI*-DMR (case 13 of group 1). This extreme hypomethylation was confirmed by bisulfite sequencing, and direct sequencing showed normal sequences of the primer-binding sites, thereby excluding the possibility that such an extremely low MI could be due to insufficient primer hybridization because of the presence of a nucleotide variation within the primer-binding sites (Figure 3). Furthermore, no copy number variation involving the *ARHI*-DMR was identified by CGH analysis using a genome-wide catalog array. Consistent with upd(7)mat, three DMRs on chromosome 7 were extremely hypermethylated in four examined cases of group 2. Only a single DMR was mildly hypermethylated in a total of 345 examined DMRs in group 3. The abnormal MIs, except for those for the *H19*-DMR in group 1 and for the three DMRs on chromosome 7 in group 2, were confirmed by three times experiments.

### Oligonucleotide array CGH

A ~3.86 Mb deletion at chromosome 17q24 was identified in a single patient (case 73 of group 3) (Figure 4).

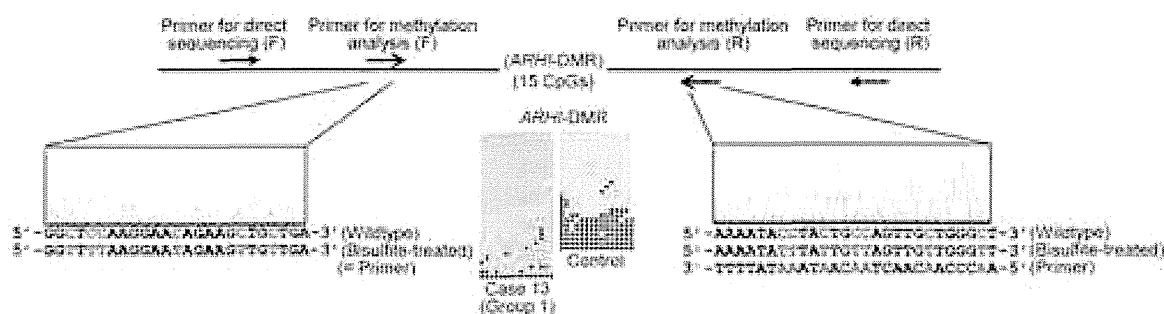


**Figure 3. Analysis of the *ARHI*-DMR in case 13.** For bisulfite sequencing, each line indicates a single clone, and each circle denotes a CpG dinucleotide; the cytosine residues at the CpG dinucleotides are usually unmethylated after paternal transmission (open circles) and methylated after maternal transmission (filled circles). Electrochromatograms delineate the sequences of the primer binding sites utilized for the methylation analysis. doi:10.1371/journal.pone.0060105.g003

### Epigenotype-phenotype analysis

Clinical findings of SRS patients in groups 1–3 are summarized in Table 2. All the patients met the mandatory criteria, and most patients in each group had severely reduced birth length and weight (both  $\leq -2$  SDS). For the five clinical features utilized as scoring system criteria, while 23.2% of patients in group 1 and 22.2% of patients in group 2 exhibited all the five features, there was no patient in group 3 who was positive for all the five features. By contrast, while 39.5% of patients in group 1 and 33.3% of patients in group 2 manifested just three of the five features, 77.6% of patients in group 3 were positive for just three features. In particular, the frequencies of relative macrocephaly at birth and body asymmetry were low in group 3, while those of the remaining three scoring system criteria including prominent forehead during early childhood were similar among groups 1–3.

Phenotypic comparison between groups 1 and 2 revealed that birth length and weight were more reduced and birth OFC was

more preserved in group 1 than in group 2, despite comparable gestational age. In the postnatal life, present height and weight became similar between the two groups, whereas present OFC became significantly smaller in group 1 than in group 2. Body asymmetry and brachydactyly were more frequent and speech delay was less frequent in group 1 than in group 2. Placental weight was similar between the two groups, and became more similar after excluding case 52 with mosaic *upd(7)mat* (see legends for Table 2). Parental age at childbirth was also similar between the two groups. In group 2, placental weight was grossly similar among examined cases, as was parental age at childbirth (see legends for Table 2).

Case 13 with an extremely low MI for the *ARHI*-DMR and case 73 with a cryptic deletion at chromosome 17q24 had no specific phenotype other than SRS-like phenotype (Table S4). However, of the five clinical features utilized as scoring system criteria, all the five features were exhibited by case 13 and just three features were

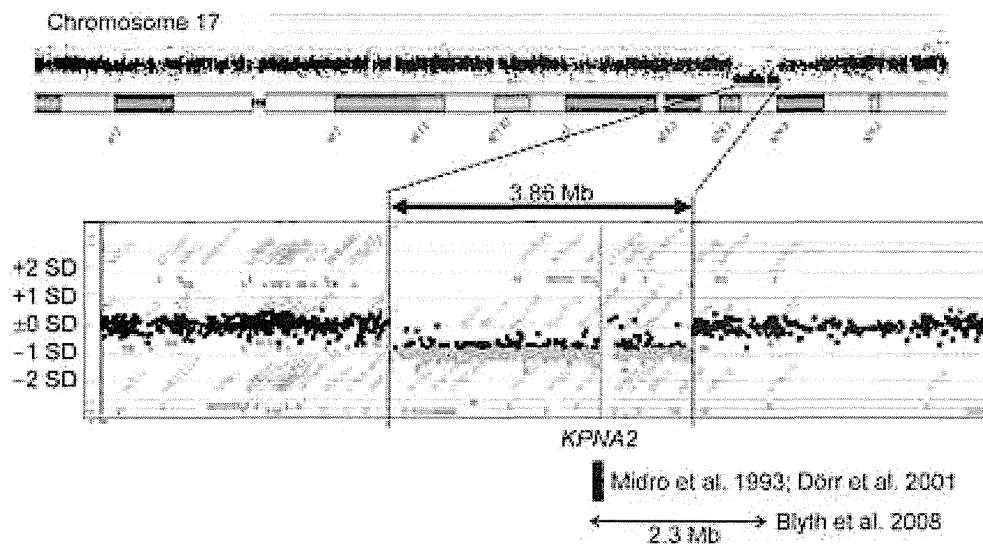


**Figure 4. Oligonucleotide array CGH in case 73, showing a ~3.86 Mb deletion at chromosome 17q24.** The black, the red, and the green dots denote signals indicative of the normal, the increased ( $> +0.5$ ), and the decreased ( $< -1.0$ ) copy numbers, respectively. The horizontal bar with arrowheads indicates a ~2.3 Mb deletion identified in a patient with Carney complex and SRS-like phenotype [44], and the black square represent a ~65 kb segment harboring the breakpoint of a *de novo* translocation 46,XY,t(1;17)(q24;q23–q24) identified in a patient with SRS phenotype [45,46]. doi:10.1371/journal.pone.0060105.g004

**Table 2.** Phenotypic comparison in three groups of patients with Silver-Russell syndrome.

	H19-DMR hypomethylation	Upd(7)mat	Unknown	P-value		
	(Group 1)	(Group 2)	(Group 3)	G1 vs. G2	G1 vs. G3	G2 vs. G3
Patient number	43 (31.2%)	9 (6.5%)	85 (62.0%)			
Mandatory criteria	43/43 (100%)	9/9 (100%)	85/85 (100%)	1.000	1.000	1.000
Scoring system criteria (5/5)	10/43 (23.2%)	2/9 (22.2%)	0/85 (0.00%)	0.965	<b>1.52 × 10<sup>-4</sup></b>	<b>2.58 × 10<sup>-2</sup></b>
Scoring system criteria (4/5)	16/43 (37.2%)	4/9 (44.4%)	19/85 (22.4%)	0.792	<b>1.45 × 10<sup>-2</sup></b>	0.145
Scoring system criteria (3/5)	17/43 (39.5%)	3/9 (33.3%)	66/85 (77.6%)	0.821	<b>7.17 × 10<sup>-4</sup></b>	0.161
Gestational age (weeks:days)	38:0 (34:3~40:0) (n=36)	38:0 (34:4~40:0) (n=9)	37:6 (27:1~41:4) (n=65)	0.877	0.120	0.450
BL (SDS)	-4.13 ± 2.01 (n=31)	-3.18 ± 1.16 (n=9)	-2.93 ± 1.43 (n=60)	<b>2.67 × 10<sup>-2</sup></b>	<b>6.69 × 10<sup>-5</sup></b>	0.619
BW (SDS)	-3.50 ± 0.85 (n=42)	-2.90 ± 0.64 (n=9)	-2.71 ± 1.14 (n=64)	<b>3.28 × 10<sup>-2</sup></b>	<b>5.87 × 10<sup>-4</sup></b>	0.640
BL ≤ -2 SDS and/or BW ≤ -2 SDS*	43/43 (100%)	9/9 (100%)	85/85 (100%)	1.000	1.000	1.000
BL ≤ -2 SDS and BW ≤ -2 SDS	39/43 (90.7%)	7/9 (77.8%)	76/85 (89.4%)	0.474	0.821	0.304
BOFC (SDS)	-0.54 ± 1.22 (n=29)	-1.44 ± 0.47 (n=9)	-1.92 ± 1.09 (n=48)	<b>3.74 × 10<sup>-2</sup></b>	<b>1.52 × 10<sup>-6</sup></b>	0.202
BL (SDS) - BOFC (SDS)	-3.70 ± 2.02 (n=27)	-1.73 ± 1.20 (n=9)	-0.943 ± 1.48 (n=43)	<b>1.02 × 10<sup>-2</sup></b>	<b>3.40 × 10<sup>-9</sup></b>	0.111
BW (SDS) - BOFC (SDS)	-3.21 ± 1.20 (n=27)	-1.53 ± 0.57 (n=9)	-1.04 ± 1.55 (n=48)	0.326	<b>7.38 × 10<sup>-9</sup></b>	0.331
Relative macrocephaly at birth† BL or BW (SDS) - BOFC (SDS) ≤ -1.5	29/29 (100%)	7/9 (77.8%)	16/45 (35.6%)	0.341	<b>3.67 × 10<sup>-8</sup></b>	<b>2.05 × 10<sup>-2</sup></b>
Present age (years:months)	4.1 (0:6~30:6) (n=31)	4.8 (2:4~25:2) (n=9)	4.3 (0:1~18:6) (n=60)	0.437	0.813	0.335
PH (SDS)	-3.58 ± 1.65 (n=35)	-3.77 ± 1.13 (n=9)	-3.17 ± 1.50 (n=61)	0.757	0.218	0.253
PH ≤ -2 SDS (≥2 years)†	29/35 (82.5%)	8/9 (88.9%)	52/61 (85.2%)	0.760	0.758	0.772
PW (SDS)	-3.15 ± 1.16 (n=32)	-2.77 ± 0.76 (n=9)	-2.77 ± 1.34 (n=59)	0.362	0.144	0.968
POFC (SDS)	-1.16 ± 1.18 (n=21)	-0.01 ± 0.91 (n=9)	-1.81 ± 1.57 (n=35)	<b>2.01 × 10<sup>-3</sup></b>	0.107	<b>3.08 × 10<sup>-3</sup></b>
PH (SDS) - POFC (SDS)	-2.47 ± 1.63 (n=16)	-3.62 ± 1.38 (n=8)	-1.55 ± 1.82 (n=35)	0.103	<b>4.39 × 10<sup>-2</sup></b>	<b>1.64 × 10<sup>-2</sup></b>
PW (SDS) - POFC (SDS)	-2.84 ± 1.31 (n=21)	-2.69 ± 1.36 (n=9)	-1.08 ± 1.71 (n=35)	0.782	<b>2.54 × 10<sup>-2</sup></b>	<b>1.90 × 10<sup>-4</sup></b>
Relative macrocephaly at present PH or PW (SDS) - POFC (SDS) ≤ -1.5	20/21 (95.2%)	8/8 (100%)	29/43 (67.4%)	0.223	<b>4.77 × 10<sup>-3</sup></b>	0.156
Triangular face during early childhood	42/43 (97.7%)	8/9 (88.9%)	65/65 (100%)	0.442	0.0773	<b>5.98 × 10<sup>-3</sup></b>
Prominent forehead during early childhood†	31/37 (83.8%)	7/9 (100%)	41/53 (77.4%)	0.200	0.456	0.978
Ear anomalies	14/35 (40.0%)	3/9 (33.3%)	15/55 (27.3%)	0.717	0.290	0.823
Irregular teeth	12/26 (46.2%)	4/9 (44.4%)	12/45 (26.7%)	0.930	0.0968	0.291
Body asymmetry†	30/37 (81.1%)	3/9 (33.3%)	19/59 (32.2%)	<b>4.77 × 10<sup>-3</sup></b>	<b>3.51 × 10<sup>-6</sup></b>	0.947
Clinodactyly	29/37 (78.4%)	5/9 (55.6%)	50/58 (86.2%)	0.167	0.323	<b>2.68 × 10<sup>-2</sup></b>
Brachydactyly	30/38 (78.9%)	2/9 (22.2%)	34/56 (60.7%)	1.16 × 10 <sup>-3</sup>	0.0642	<b>3.24 × 10<sup>-2</sup></b>
Syndactyly	3/36 (8.3%)	0/9 (0.00%)	3/52 (5.77%)	0.375	0.641	0.464
Simian crease	4/26 (15.4%)	2/7 (28.6%)	6/49 (12.2%)	0.429	0.705	0.252
Muscular hypotonia	17/32 (53.1%)	5/9 (55.6%)	12/50 (24.0%)	0.898	<b>7.49 × 10<sup>-3</sup></b>	0.0564
Developmental delay	18/37 (48.6%)	6/9 (66.7%)	25/54 (46.3%)	0.337	0.826	0.262
Speech delay	8/31 (25.8%)	6/9 (66.7%)	18/43 (41.9%)	<b>2.55 × 10<sup>-2</sup></b>	0.156	0.179
Feeding difficulty†	16/34 (47.1%)	6/9 (66.7%)	25/51 (49.0%)	0.301	0.860	0.333
Placental weight (SDS)	-2.10 ± 0.74 (n=14)	-1.72 ± 0.74 (n=6) <sup>a</sup>	-1.02 ± 0.86 (n=18)	0.312	<b>4.12 × 10<sup>-3</sup></b>	<b>8.24 × 10<sup>-3</sup></b>
Paternal age at childbirth (years:months)	32:0 (19:0~52:0) (n=24)	35:0 (27:0~48:0) (n=9)	32:0 (25:0~46:0) (n=45)	0.223	1.00	0.105
Maternal age at childbirth (years:months)	32:0 (19:0~43:0) (n=25)	33:0 (25:0~42:0) (n=9) <sup>b</sup>	30:0 (22:0~43:0) (n=46)	0.275	0.765	0.117

BL: birth length; BW: birth weight; BOFC: birth occipitofrontal circumference; PH: present height; PW: present weight; POFC: present occipitofrontal circumference, and SDS: standard deviation score.

For body features, the denominators indicate the number of patients examined for the presence or absence of each feature, and the numerators represent the number of patients assessed to be positive for that feature.

\*Mandatory criteria and five clinical features utilized as selection criteria for Silver-Russell syndrome proposed by Netchine et al. [14].

Significant P-values (<0.05) are boldfaced.

<sup>a</sup>Placental weight SDS is -1.68, -2.55, -2.24, -1.12, -2.14 and -0.60 in case 46, 47, 49, 50, 51 and 52, respectively; the placental weight SDS is -1.95 ± 0.57 in five cases except for case 52 with mosaic upd(7)mat.

<sup>b</sup>Maternal childbearing age is 32, 32, 33, 42, 32, 34, 33, 25 and 36 years in case 44-52, respectively.

doi:10.1371/journal.pone.0060105.t002

manifested by case 73. In addition, cases 136–138 with slightly elevated MIs for CG5–CG7 and CG9, and cases with multilocus methylation abnormalities, had no particular phenotype other than SRS-compatible clinical features.

### Correlation analysis

In group 1, the mean value of the MIs for CG5–CG7 and CG9 obtained by pyrosequencing analysis was positively correlated with the birth length and weight, the present height and weight, and the placental weight, but with neither the birth nor the present OFC (Table 3). Such correlations with the growth parameters were grossly similar but somewhat different for the MIs obtained by COBRA (Table S5). Furthermore, the placental weight was positively correlated with the birth weight and length, but not with the birth OFC. Such positive correlations were not found in groups 2 and 3.

### Discussion

The present study identified hypomethylation of the *H19*-DMR and *upd(7)mat* in 31.2% and 6.5% of 138 Japanese SRS patients, respectively. In this regard, the normal *KvDMR1* methylation patterns indicate that the aberrant methylation in 43 cases of group 1 is confined to the *H19*-DMR. Furthermore, oligoarray CGH excludes copy number variants involving the *H19*-DMR, and microsatellite analysis argues against segmental maternal isodisomy that could be produced by post-fertilization mitotic error [26]. These findings imply that the *H19*-DMR hypomethylation is due to epimutation (hypomethylation of the normally methylated *H19*-DMR of paternal origin).

The frequency of epimutations detected in this study is lower than that reported in Western European SRS patients [1,2,14], although the frequency of *upd(7)mat* is grossly similar between the two populations [2,11,14,27,28]. In this context, it is noteworthy that, of the five scoring system criteria, the frequencies of relative macrocephaly at birth and body asymmetry were low in group 3, while those of the remaining three scoring system criteria were similar among groups 1–3. Since relative macrocephaly and body asymmetry are characteristic of *H19*-DMR epimutation, the lack of these two features in a substantial fraction of cases in group 3 would primarily explain the low frequency of *H19*-DMR

epimutations in this study. In group 3, furthermore, the low prevalence of relative macrocephaly at birth appears to be discordant with the high prevalence of prominent forehead during early childhood. Since relative macrocephaly was evaluated by an objective method (SDS for birth length or birth weight minus SDS for birth OFC  $\leq -1.5$ ) and prominent forehead was assessed by a subjective impression of different clinicians, it is recommended to utilize relative macrocephaly as a more important and reliable feature in the scoring system than prominent forehead. In addition, the difference in the ethnic group might also be relevant to the low frequency of *H19*-DMR epimutations in this study.

Epigenotype-phenotype correlations in this study are grossly similar to those previously reported in Western European SRS patients [1–3]. Cases 1–43 in group 1 with *H19*-DMR epimutation had more reduced birth weight and length, more preserved birth OFC and more reduced present OFC, more frequent body features, and less frequent speech delay than case 44–52 in group 2 with *upd(7)mat*, although the difference in the prevalence of somatic features appears to be less remarkable in this study than in the previous studies [3,4]. This provides further support for the presence of relatively characteristic clinical features in *H19*-DMR epimutation and *upd(7)mat* [1–3]. In this context, previous studies have indicated biallelic *IGF2* expression in the human fetal choroid plexus, cerebellum, and brain, and monoallelic *IGF2* expression in the adult brain, while the precise brain tissue(s) with such a unique expression pattern remains to be clarified [29,30,31]. This may explain why the birth OFC is well preserved and the present OFC is reduced in group 1. However, since the difference in present OFC between groups 1 and 2 is not necessarily significant in the previous studies [32], the postnatal OFC growth awaits further investigations.

Placental weight was similarly reduced in groups 1 and 2. Thus, placental weight is unlikely to represent an indicator for the discrimination between the two groups, although the present data provide further support for imprinted genes being involved in placental growth, with growth-promoting effects of *PEGs* and growth-suppressing effects of *MEGs* [5,6]. It should be pointed out, however, that the placental hypoplasia could be due to some other genetic or environmental factor(s). In particular, while placental weight was apparently similar among cases of group 2, possible confined placental mosaicism [33,34] with trisomy for chromosome 7 may have exerted some effects on placental growth in cases with trisomy rescue type *upd(7)mat*.

Correlation analysis would imply that the *IGF2* expression level, as reflected by the MI of the *H19*-DMR, plays a critical role in the determination of pre- and postnatal body (stature and weight) and placental growth in patients with *H19*-DMR epimutation. Since the placental weight was positively correlated with the birth length and weight, the reduced *IGF2* expression level appears to have a similar effect on the body and the placental growth. Furthermore, the lack of correlations between the MI and birth and present OFC and between placental weight and birth OFC would be compatible with the above mentioned *IGF2* expression pattern in the central nervous system [29]. Although the MI would also reflect the *H19* expression level, this would not have a major growth effect. It has been implicated that *H19* functions as a tumor suppressor [35,36].

Multilocus analysis revealed co-existing hyper- and hypomethylated DMRs predominantly in cases of group 1, with frequencies of 35.7% of examined patients and 2.4% of examined DMRs. The results are grossly consistent with the previous data indicating that co-existing abnormal methylation patterns of DMRs are almost exclusively identified in patients with *H19*-DMR epimutation with frequencies of 9.5–30.0% of analyzed patients and 1.8–5.2% of a

**Table 3.** Correlation analyses in patients with *H19*-DMR hypomethylations.

Parameter 1	Parameter 2	r	P-value
Methylation index (%)* vs.	Birth length (SDS)	0.647	<b>6.70</b> × 10 <sup>-3</sup>
	Birth weight (SDS)	0.590	<b>7.80</b> × 10 <sup>-3</sup>
	Birth OFC (SDS)	0.190	0.498
	Present height (SDS)	0.612	<b>5.33</b> × 10 <sup>-3</sup>
	Present weight (SDS)	0.605	<b>7.81</b> × 10 <sup>-3</sup>
	Present OFC (SDS)	-0.166	0.647
Placental weight (SDS) vs.	Placental weight (SDS)	0.809	<b>8.30</b> × 10 <sup>-3</sup>
	Birth weight (SDS)	0.717	<b>8.64</b> × 10 <sup>-3</sup>
	Birth length (SDS)	0.636	<b>2.63</b> × 10 <sup>-2</sup>
	Birth OFC (SDS)	0.400	0.198

SDS: standard deviation score; and OFC: occipitofrontal circumference.

\*The mean value of MIs for CG5, CG6, CG7, and CG9 obtained by pyrosequencing analysis.

Significant P-values (<0.05) are boldfaced.

doi:10.1371/journal.pone.0060105.t003

total of analyzed DMRs [7–9]. Notably, the co-existing methylation abnormalities were predominantly observed as mild hypermethylations of maternally methylated DMRs and were restricted to a single DMR or two DMRs in patients with multilocus abnormalities. Such findings are obviously inexplicable not only by assuming a *ZFP57* mutation that is known to cause severely abnormal methylation patterns of multiple DMRs or a *ZAC1* mutation that may affect methylation patterns of multiple DMRs [37–39], but also by assuming defective maintenance of methylation in the postzygotic period [7]. Thus, some factor(s) susceptible to the co-occurrence of hypomethylation of the *H19*-DMR and hypermethylation of other DMR(s) might be operating during a gametogenic or postzygotic period in cases with *H19*-DMR epimutation.

The patients with multilocus methylation abnormalities had no specific clinical features other than SRS-compatible phenotype. Previous studies have also indicated grossly similar SRS-like phenotype between patients with monolocus and multilocus hypomethylations [7], although patients with multilocus hypomethylation occasionally have apparently severe clinical phenotype [7]. These findings would argue for the notion that the *H19*-DMR epimutation has an (epi)dominant clinical effect. Indeed, *H19*-DMR hypomethylation has led to SRS-like phenotype in a patient with parthenogenetic chimerism/mosaicism [21], whereas *H19*-DMR hypermethylation has resulted in Beckwith-Wiedemann syndrome-like phenotype in patients with androgenetic mosaicism [40].

An extremely hypomethylated *ARHI*-DMR was found in case 13. In this regard, it is known that *ARHI* with a potentially cell growth suppressor function is normally expressed from paternally inherited chromosome with unmethylated *ARHI*-DMR [41]. Indeed, hypermethylation of the *ARHI*-DMR, which is predicted to result in reduced expression of *ARHI*, has been identified as a tumorigenic factor for several cancers with an enhanced cell growth function [42,43]. Thus, it is possible that hypomethylation of the *ARHI*-DMR has led to overexpression of *ARHI*, contributing to the development of typical SRS phenotype in the presence of a low but relatively preserved MI of the *H19*-DMR in case 13.

Oligonucleotide array CGH identified a ~3.86 Mb deletion at chromosome 17q24 in case 73 of group 3. This provides further support for the presence of rare copy number variants in several SRS patients and the relevance of non-imprinted gene(s) to the development of SRS [10]. Interestingly, the microdeletion overlap with that identified in a patient with Carney complex and SRS-like features [44], and the overlapping region encompasses a ~65 kb segment defining the breakpoint of a *de novo* reciprocal translocation involving 17q23–q24 in a patient with SRS-like phenotype (Figure 4) [45,46]. Furthermore, the translocation breakage has affected *KPNA2* involved in the nuclear transport of proteins [46–48]. Thus, *KPNA2* has been regarded as a candidate gene for SRS, although mutation analysis of *KPNA2* has failed to detect a disease-causing mutation in SRS patients [49].

Lastly, it would be worth discussing on the comparison between pyrosequencing analysis and COBRA. Since the same 43 patients were found to have low MIs by both analyses, this implies that both methods can be utilized as a diagnostic tool. While the distribution of the MIs was somewhat different between the two methods, this would primarily be due to the difference in the employed methods such as the hybridization efficiency of utilized primers. Importantly, pyrosequencing analysis was capable of studying plural CpG dinucleotides at the CTCF6 binding site, whereas COBRA examined only single CpG dinucleotides outside the CTCF6 binding site. Thus, the MIs obtained by pyrosequencing analysis would be more accurate than those obtained by

COBRA in terms of *IGF2* expression levels, and this would underlie the reasonable correlations of MIs yielded by pyrosequencing analysis with body and placental growth parameters.

In summary, the present study provides useful information for the definition of molecular and clinical findings in SRS. However, several matters still remain to be elucidated, including underlying mechanisms in SRS patients with no *H19*-DMR epimutation or upd(7)mat and the DMR(s) and imprinted gene(s) responsible for the development of SRS in patients with upd(7)mat. Furthermore, while advanced maternal age at childbirth has been shown to be a predisposing factor for the development of upd(15)mat because of increased non-disjunction at meiosis I [50], such studies remain fragmentary for upd(7)mat, primarily because of the relative paucity of upd(7)mat. Further studies will permit a better characterization of SRS.

## Supporting Information

**Figure S1** Methylation analysis of the KvDMR1 using COBRA. A. Schematic representation of the KvDMR1. A 326 bp region harboring 24 CpG dinucleotides was studied. The cytosine residues at the CpG dinucleotides are usually methylated after paternal transmission (filled circles) and unmethylated after maternal transmission (open circles); after bisulfite treatment, this region is digested with *Hpy*188I when the cytosine at the 5th CpG dinucleotide (indicated with a green rectangle) is methylated and with *Eco*I when the cytosines at the 22nd CpG dinucleotide (indicated with a pink rectangle) is methylated. *KCNQ1OT1* is a paternally expressed gene, and *KCNQ1* and *CDKN1C* are maternally expressed genes. B. Representative COBRA results. U: unmethylated clone specific bands; M: methylated clone specific bands; and BWS: Beckwith-Wiedemann syndrome patient with upd(11p15)pat. C. Histograms showing the distribution of the MIs (the horizontal axis: the methylation index; and the vertical axis: the patient number). (TIF)

**Table S1** Primers utilized in the methylation analysis and microsatellite analysis. (XLS)

**Table S2** The results of microsatellite analysis. (XLSX)

**Table S3** Methylation indices for multiple differentially methylated regions (DMRs) obtained by COBRA in 38 patients with Silver-Russell syndrome. (XLSX)

**Table S4** Clinical findings in two unique patients. (DOC)

**Table S5** Correlation analyses in patients with *H19*-DMR hypomethylations. (DOC)

## Acknowledgments

We would like to thank the following doctors for providing us with blood samples and clinical data: Toshio Yamazaki, Yukihiko Hasegawa, Daisuke Ariyasu, Michiko Hayashidani, Hiroshi Yoshihashi, Tomoki Kosho, Rika Kosaki, Yasuhiro Naiki, Hideki Fujita, Aya Yamashita, Katsuhiko Maeyama, Sayu Omori, Takashi Koike, Makoto Ono, Sachiko Kitanaoka, Jun Mori, Shinichiro Miyagawa, Masamichi Ogawa, Toshiaki Tanaka, Naomi Hizuka, Yoko Fujimoto, Zenro Kizaki, Fumio Katsushima, Takashi Iwamoto, Wakako Yamamoto, Hotaka Kamasaki, Shun Soneda, Takahiro Tajima, Yoriko Watanabe, Kanako Ishii, Noriko Kinoshita, Tohyju Tanaka, Eriko Nishi, Tohru Yorifuji, Yoshio Makita, Yoshinobu Honda, Junko Tsubaki, Yoko Shimabukuro, Yoko Hiraki, Kazushige

Dobashi, Kazumichi Onigata, Hisaaki Kabata, Shigeki Ishii, Kimiko Taniguchi, and Masaoki Sugita. We are also grateful to Drs. Kyoko Tanabe and Kentaro Matsuoka for their technical assistance.

## Author Contributions

Conceived and designed the experiments: TF KY TO. Performed the experiments: TF KN CT S. Sano K. Matsubara MK KY. Analyzed the data: TF KN KH KY. Contributed reagents/materials/analysis tools: SM TN TH RH YM K. Muroya TK CN S. Sato TO. Wrote the paper: TO.

## References

- Eggermann T (2010) Russell-Silver syndrome. *Am J Med Genet C Semin Med Genet* 154C: 355–364.
- Binder G, Begemann M, Eggermann T, Kannenberg K (2011) Silver-Russell syndrome. *Best Pract Res Clin Endocrinol Metab* 25: 153–160.
- Wakeling EL, Amero SA, Alders M, Bliok J, Forsythe E, et al. (2010) Epigenotype-phenotype correlations in Silver-Russell syndrome. *J Med Genet* 47: 760–768.
- Yamazawa K, Kagami M, Nagai T, Kondoh T, Onigata K, et al. (2008) Molecular and clinical findings and their correlations in Silver-Russell syndrome: implications for a positive role of IGF2 in growth determination and differential imprinting regulation of the IGF2-H19 domain in bodies and placentas. *J Mol Med (Berl)* 86: 1171–1181.
- Fowden AL, Sibley C, Reik W, Constancia M (2006) Imprinted genes, placental development and fetal growth. *Horm Res* 65 Suppl 3: 50–58.
- Yamazawa K, Kagami M, Ogawa M, Horikawa R, Ogata T (2008) Placental hypoplasia in maternal uniparental disomy for chromosome 7. *Am J Med Genet A* 146A: 514–516.
- Azzi S, Rossignol S, Steunou V, Sas T, Thibaud N, et al. (2009) Multilocus methylation analysis in a large cohort of 11p15-related foetal growth disorders (Russell Silver and Beckwith Wiedemann syndromes) reveals simultaneous loss of methylation at paternal and maternal imprinted loci. *Hum Mol Genet* 18: 4724–4733.
- Turner CL, Mackay DM, Callaway JL, Docherty LE, Poole RL, et al. (2010) Methylation analysis of 79 patients with growth restriction reveals novel patterns of methylation change at imprinted loci. *Eur J Hum Genet* 18: 648–655.
- Hiura H, Okae H, Miyauchi N, Sato F, Sato A, et al. (2012) Characterization of DNA methylation errors in patients with imprinting disorders conceived by assisted reproduction technologies. *Hum Reprod* 27: 2541–2548.
- Abu-Amro S, Monk D, Frost J, Preece M, Stanier P, et al. (2008) The genetic aetiology of Silver-Russell syndrome. *J Med Genet* 45: 193–199.
- Hitchins MP, Stanier P, Preece MA, Moore GE (2001) Silver-Russell syndrome: a dissection of the genetic aetiology and candidate chromosomal regions. *J Med Genet* 38: 810–819.
- Spengler S, Schönherr N, Binder G, Wollmann HA, Fricke-Otto S, et al. (2010) Submicroscopic chromosomal imbalances in idiopathic Silver-Russell syndrome (SRS): the SRS phenotype overlaps with the 12q14 microdeletion syndrome. *J Med Genet* 47: 356–360.
- Fuke-Sato T, Yamazawa K, Nakabayashi K, Matsubara K, Matsuoka K, et al. (2012) Mosaic upd(7)mat in a patient with Silver-Russell syndrome. *Am J Med Genet A* 158A: 465–468.
- Netchine I, Rossignol S, Dufourg MN, Azzi S, Rousseau A, et al. (2007) 11p15 imprinting center region 1 loss of methylation is a common and specific cause of typical Russell-Silver syndrome: clinical scoring system and epigenetic-phenotypic correlations. *J Clin Endocrinol Metab* 92: 3148–3154.
- Kagami M, Yamazawa K, Matsubara K, Matsuo N, Ogata T (2008) Placentomegaly in paternal uniparental disomy for human chromosome 14. *Placenta* 29: 760–761.
- Bell AC, Felsenfeld G (2000) Methylation of a CTCF-dependent boundary controls imprinted expression of the *Igf2* gene. *Nature* 405: 482–485.
- Hark AT, Schoenherr CJ, Katz DJ, Ingram RS, Levorse JM, et al. (2000) CTCF mediates methylation-sensitive enhancer-blocking activity at the H19/*Igf2* locus. *Nature* 405: 486–489.
- Takai D, Gonzales FA, Tsai YC, Thayer MJ, Jones PA (2001) Large scale mapping of methylcytosines in CTCF-binding sites in the human H19 promoter and aberrant hypomethylation in human bladder cancer. *Hum Mol Genet* 10: 2619–2626.
- Fisher AM, Thomas NS, Cockwell A, Stecko O, Kerr B, et al. (2002) Duplications of chromosome 11p15 of maternal origin result in a phenotype that includes growth retardation. *Hum Genet* 111: 290–296.
- Brena RM, Auer H, Kornacker K, Hackanson B, Raval A, et al. (2006) Accurate quantification of DNA methylation using combined bisulfite restriction analysis coupled with the Agilent 2100 Bioanalyzer platform. *Nucleic Acids Res* 34: e17.
- Yamazawa K, Nakabayashi K, Kagami M, Sato T, Saitoh S, et al. (2010) Parthenogenetic chimaerism/mosaicism with a Silver-Russell syndrome-like phenotype. *J Med Genet* 47: 782–785.
- Shaffer LG, Agan N, Goldberg JD, Ledbetter DH, Longshore JW, et al. (2001) American College of Medical Genetics statement on diagnostic testing for uniparental disomy. *Genet Med* 3: 206–211.
- Hannula K, Lipsanen-Nyman M, Kontiokari T, Kere J (2001) A narrow segment of maternal uniparental disomy of chromosome 7q31-qter in Silver-Russell syndrome delimits a candidate gene region. *Am J Hum Genet* 68: 247–253.
- Eggermann T, Schonherr N, Jager S, Spaich C, Ranke MB, et al. (2008) Segmental maternal UPD(7q) in Silver-Russell syndrome. *Clin Genet* 74: 486–489.
- Begemann M, Spengler S, Kordass U, Schroder C, Eggermann T (2012) Segmental maternal uniparental disomy 7q associated with DLK1/GTL2 (14q32) hypomethylation. *Am J Med Genet A* 158A: 423–428.
- Yamazawa K, Ogata T, Ferguson-Smith AC (2010) Uniparental Disomy and Human Disease: An Overview. *Am J Med Genet C* 154C: 329–334.
- Gicquel C, Rossignol S, Cabrol S, Houang M, Steunou V, et al. (2005) Epimutation of the telomeric imprinting center region on chromosome 11p15 in Silver-Russell syndrome. *Nat Genet* 37: 1003–1007.
- Bliok J, Terhal P, van den Bogaard MJ, Maas S, Hamel B, et al. (2006) Hypomethylation of the H19 gene causes not only Silver-Russell syndrome (SRS) but also isolated asymmetry or an SRS-like phenotype. *Am J Hum Genet* 78: 604–614.
- Ulaner GA, Yang Y, Hu JF, Li T, Vu TH, et al. (2003) CTCF binding at the insulin-like growth factor-II (IGF2)/H19 imprinting control region is insufficient to regulate IGF2/H19 expression in human tissues. *Endocrinology* 144: 4420–4426.
- Pham NV, Nguyen MT, Hu JF, Vu TH, Hoffman AR (1998) Dissociation of IGF2 and H19 imprinting in human brain. *Brain Res* 810: 1–8.
- Albrecht S, Waha A, Koch A, Kraus JA, Goodyer CG, et al. (1996) Variable imprinting of H19 and IGF2 in fetal cerebellum and medulloblastoma. *J Neuropathol Exp Neurol* 55: 1270–1276.
- Kotzot D (2008) Maternal uniparental disomy 7 and Silver-Russell syndrome - clinical update and comparison with other subgroups. *Eur J Med Genet* 51: 444–451.
- Kotzot D, Balmer D, Baumer A, Chrzanowska K, Hamel BC, et al. (2000) Maternal uniparental disomy 7-review and further delineation of the phenotype. *Eur J Pediatr* 159: 247–256.
- Robinson WP (2000) Mechanisms leading to uniparental disomy and their clinical consequences. *Bioessays* 22: 452–459.
- Hao Y, Crenshaw T, Moulton T, Newcomb E, Tycko B (1993) Tumour-suppressor activity of H19 RNA. *Nature* 365: 764–767.
- Juan V, Crain C, Wilson C (2000) Evidence for evolutionarily conserved secondary structure in the H19 tumor suppressor RNA. *Nucleic Acids Res* 28: 1221–1227.
- Arima T, Kamikihara T, Hayashida T, Kato K, Inoue T, et al. (2005) ZAC, LIT1 (KCNQ1OT1) and p57KIP2 (CDKN1C) are in an imprinted gene network that may play a role in Beckwith-Wiedemann syndrome. *Nucleic Acids Res* 33: 2650–2660.
- Varrault A, Gueydan C, Delalbre A, Bellmann A, Houssami S, et al. (2006) Zac1 regulates an imprinted gene network critically involved in the control of embryonic growth. *Dev Cell* 11: 711–722.
- Quenneville S, Verde G, Corsinotti A, Kapopoulou A, Jakobsson J, et al. (2011) In embryonic stem cells, ZFP57/KAP1 recognize a methylated hexanucleotide to affect chromatin and DNA methylation of imprinting control regions. *Mol Cell* 44: 361–372.
- Yamazawa K, Nakabayashi K, Matsuoka K, Masubara K, Hata K, et al. (2011) Androgenetic/biparental mosaicism in a girl with Beckwith-Wiedemann syndrome-like and upd(14)pat-like phenotypes. *J Hum Genet* 56: 91–93.
- Huang J, Lin Y, Li L, Qing D, Teng XM, et al. (2009) ARHI, as a novel suppressor of cell growth and downregulated in human hepatocellular carcinoma, could contribute to hepatocarcinogenesis. *Mol Carcinog* 48: 130–140.
- Feng W, Marquez RT, Lu Z, Liu J, Lu KH, et al. (2008) Imprinted tumor suppressor genes ARHI and PEG3 are the most frequently down-regulated in human ovarian cancers by loss of heterozygosity and promoter methylation. *Cancer* 112: 1489–1502.
- Tang HL, Hu YQ, Qin XP, Jazag A, Yang H, et al. (2012) Aplasia ras homolog member 1 is downregulated in gastric cancer and silencing its expression promotes cell growth in vitro. *J Gastroenterol Hepatol* 27: 1395–1404.
- Blyth M, Huang S, Maloney V, Crolla JA, Karen Temple I (2008) A 2.3 Mb deletion of 17q24.2-q24.3 associated with 'Carney Complex plus'. *Eur J Med Genet* 51: 672–678.
- Midro AT, Debek K, Sawicka A, Marcinkiewicz D, Rogowska M (1993) Second observation of Silver-Russell syndrome in a carrier of a reciprocal translocation with one breakpoint at site 17q25. *Clin Genet* 44: 53–55.
- Dörr S, Midro AT, Farber C, Giannakudis J, Hansmann I (2001) Construction of a detailed physical and transcript map of the candidate region for Russell-Silver syndrome on chromosome 17q23-q24. *Genomics* 71: 174–181.
- Cuomo CA, Kirch SA, Gyuris J, Brent R, Oettinger MA (1994) Rch1, a protein that specifically interacts with the RAG-1 recombination-activating protein. *Proc Natl Acad Sci U S A* 91: 6156–6160.

48. Weis K, Mattaj JW, Lamond AI (1995) Identification of hSRP1 alpha as a functional receptor for nuclear localization sequences. *Science* 268: 1049–1053.
49. Dörr S, Schlicker M, Hansmann I (2001) Genomic structure of karyopherin alpha2 (KPNA2) within a low-copy repeat on chromosome 17q23-q24 and mutation analysis in patients with Russell-Silver syndrome. *Hum Genet* 109: 479–486.
50. Matsubara K, Murakami N, Nagai T, Ogata T (2011) Maternal age effect on the development of Prader-Willi syndrome resulting from upd(15)mat through meiosis I errors. *J Hum Genet* 56: 566–571.

# A Loss-of-Function Mutation in the *SLC9A6* Gene Causes X-Linked Mental Retardation Resembling Angelman Syndrome

Yumi Takahashi,<sup>1</sup> Kana Hosoki,<sup>1</sup> Masafumi Matsushita,<sup>2</sup> Makoto Funatsuka,<sup>3</sup> Kayoko Saito,<sup>4</sup> Hiroshi Kanazawa,<sup>2</sup> Yu-ichi Goto,<sup>5</sup> and Shinji Saitoh<sup>1\*</sup>

<sup>1</sup>Department of Pediatrics, Hokkaido University Graduate School of Medicine, Sapporo, Japan

<sup>2</sup>Department of Biological Sciences, Graduate School of Science, Osaka University, Osaka, Japan

<sup>3</sup>Department of Pediatrics, Tokyo Womens' Medical University, Tokyo, Japan

<sup>4</sup>Institute of Medical Genetics, Tokyo Womens' Medical University, Tokyo, Japan

<sup>5</sup>Department of Mental Retardation and Birth Defect Research, National Institute of Neuroscience, National Center of Neurology and Psychiatry, Tokyo, Japan

Received 29 November 2010; Accepted 6 July 2011

*SLC9A6* mutations have been reported in families in whom X-linked mental retardation (XMR) mimics Angelman syndrome (AS). However, the relative importance of *SLC9A6* mutations in patients with an AS-like phenotype or XMR has not been fully investigated. Here, the involvement of *SLC9A6* mutations in 22 males initially suspected to have AS but found on genetic testing not to have AS (AS-like cohort), and 104 male patients with XMR (XMR cohort), was investigated. A novel *SLC9A6* mutation (c.441delG, p.S147fs) was identified in one patient in the AS-like cohort, but no mutation was identified in XMR cohort, suggesting mutations in *SLC9A6* are not a major cause of the AS-like phenotype or XMR. The patient with the *SLC9A6* mutation showed the typical AS phenotype, further demonstrating the similarity between patients with AS and those with *SLC9A6* mutations. To clarify the effect of the *SLC9A6* mutation, we performed RT-PCR and Western blot analysis on lymphoblastoid cells from the patient. Expression of the mutated transcript was significantly reduced, but was restored by cycloheximide treatment, indicating the presence of nonsense mediated mRNA decay. Western blot analysis demonstrated absence of the normal NHE6 protein encoded for by *SLC9A6*. Taken together, these findings indicate a loss-of-function mutation in *SLC9A6* caused the phenotype in our patient. © 2011 Wiley-Liss, Inc.

**Key words:** *SLC9A6*; sodium/hydrogen exchanger 6; Angelman syndrome; X-linked mental retardation; nonsense mediated mRNA decay

## INTRODUCTION

*SLC9A6* mutations were first reported by Gilfillan et al. [2008] in families exhibiting an X-linked mental retardation (XMR) syndrome mimicking Angelman syndrome (AS). Angelman syndrome is characterized by severe developmental delay with absent or minimal speech, ataxia, easily provoked laughter, epilepsy, and

### How to Cite this Article:

Takahashi Y, Hosoki K, Matsushita M, Funatsuka M, Saito K, Kanazawa H, Goto Y-I, Saitoh S. 2011. A Loss-of-Function Mutation in the *SLC9A6* Gene Causes X-Linked Mental Retardation Resembling Angelman Syndrome.

Am J Med Genet Part B 156:799–807.

microcephaly. The syndrome is caused by loss-of-function of the *UBE3A* gene which is subject to genomic imprinting. Patients with *SLC9A6* mutations resemble patients with AS, but also demonstrate distinctive clinical features including cerebellar atrophy, slow progression of symptoms, increased glutamate/glutamic acid peak on magnetic resonance spectroscopy (MRS), and lack of characteristic abnormalities seen AS patients examined using electroencephalography (EEG). Following the first report in 2008, in 2010 Schroer et al. reported two other families with AS due to *SLC9A6* mutations, and confirmed the findings of Gilfillan et al.

The *SLC9A6* gene is located on Xq26.3, and encodes the ubiquitously expressed Na<sup>+</sup>/H<sup>+</sup> exchanger protein member 6, NHE6. The NHE protein family consists of nine members and includes

Grant sponsor: Ministry of Education, Culture, Sports, Science, and Technology, Japan; Grant number: 21591306.

\*Correspondence to:

Shinji Saitoh, Department of Pediatrics, Hokkaido University Graduate School of Medicine, N-15, W-7, Kita-ku, Sapporo 060-8638, Japan.

E-mail: ss11@med.hokudai.ac.jp

Published online 2 August 2011 in Wiley Online Library (wileyonlinelibrary.com).

DOI 10.1002/ajmg.b.31221

NHE1-5 which is found in the plasma membrane, and NHE6-9 which is found in the membranes of intracellular organelles such as mitochondria and endosomes. NHE6 is predominantly present in the early recycling endosome membranes, and is believed to have a role in regulating luminal pH and monovalent cation concentration in intracellular organelles [Brett et al., 2002; Nakamura et al., 2005]. Moreover, Roxrud et al. demonstrated that NHE6 in combination with NHE9 participated in regulation of endosomal pH in HeLa cells by means of the procedure of co-depletion of NHE6 and NHE9 [Roxrud et al. 2009], indicating the significant role of NHE6 in fine-tuning of endosomal pH in human cells. In the brain, exocytosis from recycling endosomes is essential for the growth of dendritic spines which grow during long-term potentiation (LTP). In the absence of recycling endosomal transport, spines are rapidly lost, and LTP stimuli fail to elicit spine growth [Park et al., 2006]. Thus, NHE6 has an important role in the growth of dendritic spines, and also in the development of normal brain wiring. Thus far, five *SLC9A6* mutations have been reported in six AS families; two nonsense mutations, one inframe deletion, one frameshift deletion, and one splicing mutation [Gilfillan et al., 2008; Schroer et al., 2010]. The precise pathogenesis by which these mutations produce disease remains to be clarified.

The aim of this study was to clarify the incidence and importance of *SLC9A6* mutations in AS-like patients and patients with XMR, and to shed light on the molecular pathogenesis of disease due to *SLC9A6* mutations.

## MATERIALS AND METHODS

### Enrolled Patients

We examined 22 affected Japanese males clinically suspected of having AS but who lacked the genetic abnormalities reported in AS (AS-like cohort). These patients had AS excluded by having negative results for the *SNURF-SNRPN* DNA methylation test (which identifies a deletion, uniparental disomy, or imprinting defect) and *UBE3A* mutation screening (performed as described previously) [Saitoh et al., 2005]. We also examined DNA samples from 104 Japanese patients suspected of having XMR (XMR cohort). The XMR samples were collected as a part of a project for the Japanese Mental Retardation Consortium [Takano et al., 2008]. This study was approved by the Institutional Review Board of Hokkaido University Graduate School of Medicine, and written informed consent was obtained from the parents of the enrolled patients.

### Mutation Analysis of the *SLC9A6* Gene

We amplified each exon, including exon–intron boundaries, of the *SLC9A6* gene using polymerase chain reaction (PCR), and all amplicons were directly sequenced on an ABI 3130 DNA analyzer (Applied Biosystems, Foster City, CA) using BigDye Terminator V.1.1 Cycle Sequencing Kit (Applied Biosystems). *SLC9A6* encodes two alternatively spliced transcripts produced from alternative splicing donor sites in exon 2 which give rise to a long form designated as variant 1, and a short form called variant 2. Variant 1 and variant 2 code for NHE6.1 (isoform a) and NHE6.0 (isoform b), respectively (Fig. 1). The primers were designed to amplify each transcript variant. The primers sequence used for amplification and

sequencing are available on request. Genomic DNA (10 ng) extracted from peripheral blood was amplified in a total PCR volume of 20  $\mu$ l containing 1 $\times$  buffer, 0.4  $\mu$ M of each primer (forward/reverse), 0.18 mM dNTPs, 0.5 U AmpliTaq Gold<sup>®</sup> DNA Polymerase (Applied Biosystems). The PCRs for all exons except exon one were performed at 94°C for 10 min followed by 30 cycles of 94°C for 30 sec, 55°C for 30 sec, 72°C for 30 sec, then one cycle at 72°C for 7 min. The high CpG content of exon 1 required it to be amplified in a total reaction volume of 20  $\mu$ l containing 1 $\times$  buffer, 0.4  $\mu$ M of each primer, 0.2 mM dNTPs, 0.4 U Phusion<sup>®</sup> Hot Start High-Fidelity DNA Polymerase (Finnzymes, Vantaa, Finland), and 3% DMSO. The thermocycling conditions for exon 1 were 98°C for 3 min followed by 35 cycles of 98°C for 10 sec, 65°C for 30 sec and 72°C for 30 sec and then one cycle of 72°C for 5 min. The PCR products were purified with Wizard<sup>®</sup> PCR Preps DNA Purification System (Promega, Madison, WI) prior to sequencing. All mutations are referred to in relation to reference sequence NM\_001042537.

### Cell Culture and Cycloheximide Treatment

Epstein–Barr virus (EBV)-transformed lymphoblastoid cells lines were established from peripheral blood cells using standard methods. To prevent potential degradation of transcripts containing premature translation termination codons (PTCs) by nonsense mediated mRNA decay (NMD), lymphoblastoid cells from the patient with the *SLC9A6* mutation and normal controls were treated with 100  $\mu$ g/ml cycloheximide (CHX) (Sigma, St. Louis, MO). This compound interferes with NMD through inhibition of protein synthesis [Aznarez et al., 2007]. CHX or a 0.1% DMSO control vehicle was used 4 hr prior to RNA extraction from the cell lines [Carter et al., 1995].

### RT-PCR

Total RNA from cultured lymphoblastoid cells from the patient and four normal controls, was extracted using the RNAqueous<sup>®</sup> Kit (Applied Biosystems). Reverse transcription was performed using 100 ng of total RNA and the High-Capacity cDNA Reverse Transcription Kit (Applied Biosystems) in a total reaction volume of 20  $\mu$ l containing 1 $\times$  Random primers, 4 mM dNTP mix, 2.5 U of Multiscribe<sup>™</sup> Reverse Transcriptase, and 1  $\mu$ l of RNase Inhibitor. The reactions were incubated at 25°C for 10 min, then at 37°C for 120 min and then followed by 85°C for 5 min to inactivate the reverse transcriptase. Complementary DNA was then amplified using a primer set designed to amplify exon 2–5; forward 5'-GTCTTTTGGTGGGCCTTGT-3', reverse 5'-GTCCCGTTACCTTCATCAG-3'. PCR products for NHE6.1 (transcript variant 1) and NHE6.0 (transcript variant 2) were 399 and 303 bp, respectively.

### Real-Time Quantification of *SLC9A6* mRNA

To measure *SLC9A6* transcript variant 1 and variant 2, both of which are alternative splicing products, primers and TaqMan<sup>®</sup> MGB probes were designed with Primer<sup>®</sup> Express Software (Applied Biosystems; Fig. 1). The Primer and MGB probe sequence

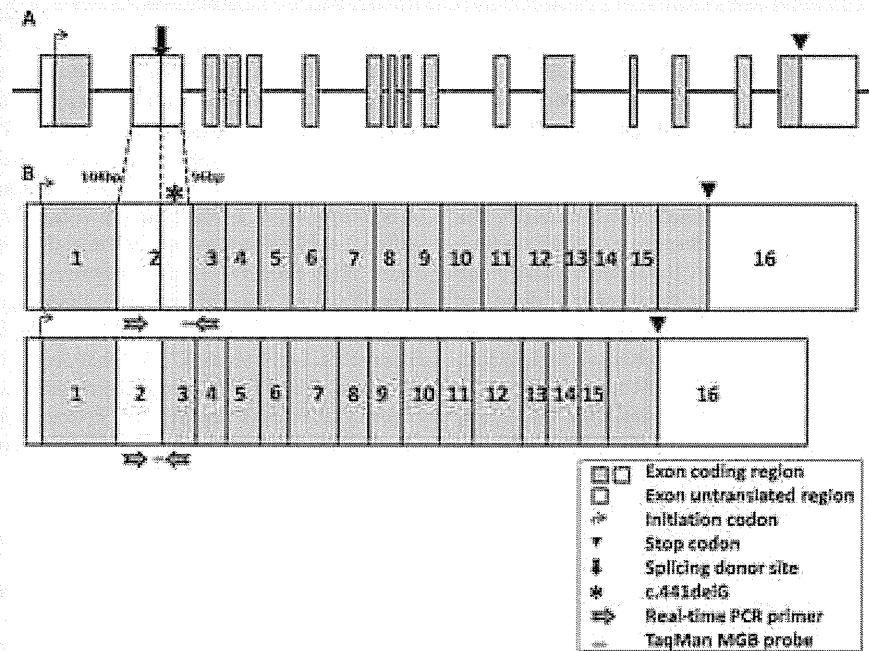


FIG. 1. A: Genomic structure of the *SLC9A6* gene. B: Two alternatively spliced transcripts of the *SLC9A6* gene. Above: *SLC9A6* transcript variant 1 (encodes NHE6.1 or isoform a). Below: *SLC9A6* transcript variant 2 (encodes NHE6.0 or isoform b). The location of the *SLC9A6* mutation in our patient is shown with \*. Primers and probes used in real-time quantitative PCR are shown (horizontal arrows).

for variant 1 were forward primer 5'-TGAGTATATGCTG-AAAGGAGAGATTAGTTC-3', reverse primer 5'-GATAGGAGGAAGTAATATGTTGAAAAATACTTC-3', TaqMan MGB probe 5'-CTTAGAAAGGTTACTTTTGGATCC-3'; and for variant 2 forward primer 5'-CTGTGAAGTGCAGTCAAGTCCAA-3', reverse primer 5'-GATAGGAGGAAGTAATATGTTGAAAAATACTTC-3', TaqMan MGB probe 5'-CTACCTTACTGGTTACTTTTGA-3'. Human *GAPDH* MGB probe and primers purchased from Applied Biosystems were used as the internal control. Patient cDNA was transcribed from 10 ng of total RNA in a total volume of 25  $\mu$ l containing 1  $\times$  TaqMan<sup>®</sup> Universal PCR Master Mix (Applied Biosystems), 0.9  $\mu$ M of each primer (sense/antisense) and 0.25  $\mu$ M of probe. Thermocycling was 95°C for 10 min, followed by 40 cycles of 95°C for 15 sec and 60°C for 1 min. Real-time quantitative PCR was performed using the ABI PRISM 7700 (Applied Biosystems). The  $2^{-\Delta\Delta C_t}$  method was used for relative quantification.

### Western Blot Analysis

HeLa cells and cultured lymphoblastoid cells from the patient, mother and normal controls were washed with phosphate buffered saline and suspended in lysis buffer (phosphate buffered saline containing 1% Triton-X, 1  $\mu$ g/ml aprotinin, 1  $\mu$ g/ml pepstatin A, and 1  $\mu$ g/ml leupeptin). HeLa cells expressing the NHE6.1 were used as a control. The cells were disrupted by sonication and

centrifuged at 20,000g for 10 min at 4°C. The supernatants were then resolved by SDS-polyacrylamide electrophoresis and transferred to polyvinylidene fluoride membrane (Millipore, Billerica, MA). NHE6 was detected with rabbit polyclonal anti-NHE6 antibody [Ohgaki et al., 2008], anti-rabbit IgG antibody conjugated with horseradish peroxidase (Vector Laboratories, Burlingame, CA) and chemiluminescence reagent (ECL Western Blotting Detection System; GE Healthcare, Waukesha, WI).

## RESULTS

### Identification of a *SLC9A6* Mutation

We identified only one male patient with a frameshift mutation (c.441delG, p.S147fs) in exon 2, out of 22 male patients in the AS-like cohort (Fig. 2). This frameshift mutation causes a PTC. His healthy mother was heterozygous for the mutation.

No mutation in the *SLC9A6* gene was identified in the XMR cohort. However, two common polymorphisms (rs2291639, rs2307131), and one putative novel polymorphism in intron 12 (c.1692 +10 A>G) were detected.

### Clinical Features of the Patient With the *SLC9A6* Mutation

The affected male patient at birth suffered from mild neonatal asphyxia, however he had no other perinatal problems. His parents

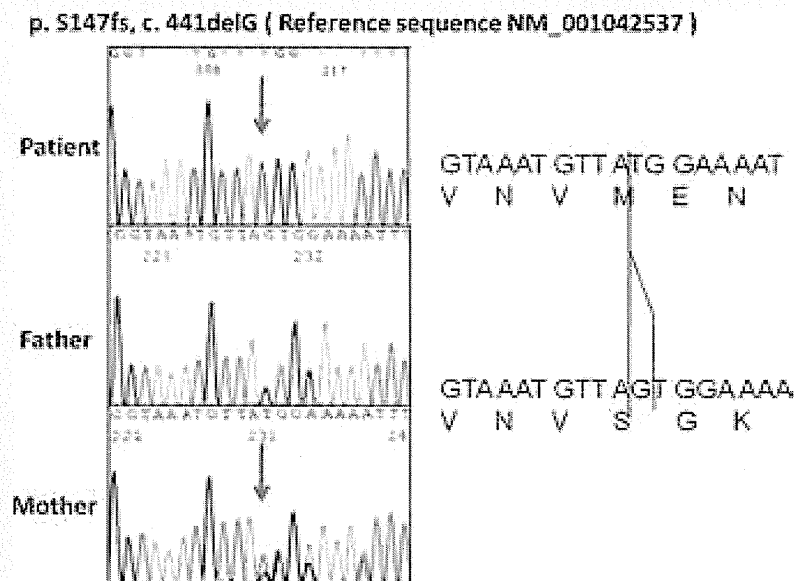


**FIG. 2.** Chromatographs showing the *SLC9A6* mutation in our patient, and the equivalent genomic region in both his parents. The mutation c.441delG is located in exon 2 and is only present in transcript variant 1. His mother was heterozygous for this mutation, while his father did not have the mutation. This mutant transcript leads to premature protein truncation. The mutation is described relative to reference sequence NM\_001043537. [Color figure can be seen in the online version of this article, available at [http://onlinelibrary.wiley.com/journal/10.1002/\(ISSN\)1552-485X](http://onlinelibrary.wiley.com/journal/10.1002/(ISSN)1552-485X)]

were non-consanguineous and he did not have any family history of neurological diseases. Although formal clinical assessment was not conducted to the mother, she is healthy and does not have intellectual disability. His clinical features are summarized in Table I. He showed typical findings of AS; severe developmental delay with absence of verbal language, generalized hypotonia, easily provoked laughter, epilepsy, ataxia, strabismus, and microcephaly. His occipitofrontal head circumference at birth was 33.8 cm (+0.4 SD), but his head growth has decelerated into 51.5 cm (−3.0 SD) at 18 years of age. He acquired head control at three months of age, sat and crawled at 6 months of age, and walked unassisted at 18 months of age. His first epileptic attack occurred at 4 years of age. After this first attack, he lost his ability to walk until he was 5 years old. His epileptic attacks consisted of multiple types of seizures, and they were difficult to control with ACTH or several anti-epileptic drugs. TRH treatment improved his awakening and activity levels, and he transiently acquired the ability to walk. However, subsequently his ability to walk was lost, probably due to exacerbation of ataxia. His deep tendon reflex was not increased and no other features of spasticity or peripheral neuropathy were identified. His EEG findings included a background frequency of 5–6 Hz theta waves and spontaneous appearance of 3 Hz diffuse high voltage slow waves. TRH did not change the frequency of his seizures or his EEG findings. He showed no cerebellar atrophy on magnetic resonance imaging (MRI) at 5 years of age. MRS was not performed. He had a normal G-banding karyotype.

#### Downregulation of the *SLC9A6* Variant 1 in the Patient With the Mutation

The identified mutation c.441delG is located in exon 2 and is only present in variant 1 (Fig. 1). Therefore, the mutation only affects NHE6.1, leaving NHE6.0 intact. Reverse transcriptase PCR demonstrated that *SLC9A6* variant 1 mRNA expression decreased in our patient (Fig. 3A) compared to that in four normal controls. On the other hand, variant 2 expression was increased in the patient compared to the controls. To further investigate mutant *SLC9A6* gene expression, real-time quantitative PCR (qPCR) was performed using cDNA from the patient and normal controls. Quantitative PCR confirmed that *SLC9A6* variant 1 was significantly downregulated in the patient, while it was not downregulated in normal controls (Fig. 4A). Furthermore, the *SLC9A6* variant 2 mRNA in the patient was significantly increased compared to normal controls (Fig. 4B).

#### Nonsense Mediated Decay Was Involved in the Downregulation of Mutant *SLC9A6* in the Patient

To investigate the possible involvement of NMD in the downregulation of mutant *SLC9A6* in the patient's lymphoblastoid cells, we treated the cells with CHX. After CHX treatment, the expression level of *SLC9A6* variant 1 increased compared to normal control samples on RT-PCR (Fig. 3B). It was also proved that the expression level of variant 1 was significantly increased by performing qPCR, while the expression level in normal control samples